

GPR37 expression as a prognostic marker in gliomas: a bioinformatics-based analysis

Kairong Liang^{1,*}, Zhaoxiong Guo^{2,*}, Shizhen Zhang^{1,*}, Danmin Chen¹, Renheng Zou¹, Yuhao Weng¹, Chengxiang Peng¹, Zhichao Xu¹, Jingbai Zhang¹, Xiaorui Liu⁴, Xiao Pang¹, Yunxiang Ji¹, Degui Liao¹, Miaoling Lai¹, Huaidong Peng³, Yanbin Ke¹, Zhaotao Wang¹, Yezhong Wang¹

¹Institute of Neuroscience, Department of Neurosurgery, The Second Affiliated Hospital of Guangzhou Medical University, Guangzhou 510260, China

²Science and Technology Innovation Center, Institute of Clinical Pharmacology, Guangzhou University of Chinese Medicine, Guangzhou 510405, China

³Department of Pharmacy, The Second Affiliated Hospital of Guangzhou Medical University, Guangzhou 510260, China

⁴Department of Pharmacy, Affiliated Cancer Hospital and Institute of Guangzhou Medical University, Guangzhou 510095, China

*Equal contribution

Correspondence to: Zhaotao Wang, Yezhong Wang, Yanbin Ke; **email:** wangzhaotao@gzhmu.edu.cn; wangyezong@gzhmu.edu.cn; 14729585@qq.com, <https://orcid.org/0009-0003-6416-7651>

Keywords: glioma, *GPR37*, prognosis, immune infiltration, M2 macrophages

Received: April 18, 2023

Accepted: August 21, 2023

Published: October 13, 2023

Copyright: © 2023 Liang et al. This is an open access article distributed under the terms of the [Creative Commons Attribution License](https://creativecommons.org/licenses/by/3.0/) (CC BY 3.0), which permits unrestricted use, distribution, and reproduction in any medium, provided the original author and source are credited.

ABSTRACT

Background: Gliomas are the most frequently diagnosed primary brain tumors, and are associated with multiple molecular aberrations during their development and progression. *GPR37* is an orphan G protein-coupled receptor (GPCR) that is implicated in different physiological pathways in the brain, and has been linked to various malignancies. The aim of this study was to explore the relationship between *GPR37* gene expression and the clinicopathological factors, patient prognosis, tumor-infiltrating immune cell signature GSEA and methylation levels in glioma.

Methods: We explored the diagnostic value, clinical relevance, and molecular function of *GPR37* in glioma using TCGA, STRING, cBioPortal, Tumor Immunity Estimation Resource (TIMER) database and MethSurv databases. Besides, the "ssGSEA" algorithm was conducted to estimate immune cells infiltration abundance, with 'ggplot2' package visualizing the results. Immunohistochemical staining of clinical samples were used to verify the speculations of bioinformatics analysis.

Results: *GPR37* expression was significantly higher in the glioma tissues compared to the normal brain tissues, and was linked to poor prognosis. Functional annotation of *GPR37* showed enrichment of ether lipid metabolism, fat digestion and absorption, and histidine metabolism. In addition, GSEA showed that *GPR37* was positively correlated to the positive regulation of macrophage derived foam cell differentiation, negative regulation of T cell receptor signaling pathway, neuroactive ligand receptor interaction, calcium signaling pathway, and negatively associated with immunoglobulin complex, immunoglobulin complex circulating, ribosome and spliceosome mediated by circulating immunoglobulin etc. TIMER2.0 and ssGSEA showed that *GPR37* expression was significantly associated with the infiltration of T cells, CD8 T cell, eosinophils, macrophages, neutrophils, NK CD56^{dim} cells, NK cells, plasmacytoid DCs (pDCs), T helper cells and T effector

memory (Tem) cells. In addition, high *GPR37* expression was positively correlated with increased infiltration of M2 macrophages, which in turn was associated with poor prognosis. Furthermore, *GPR37* was positively correlated with various immune checkpoints (ICPs). Finally, hypomethylation of the *GPR37* promoter was associated with its high expression levels and poor prognosis in glioma.

Conclusion: *GPR37* had diagnostic and prognostic value in glioma. The possible biological mechanisms of *GPR37* provide novel insights into the clinical diagnosis and treatment of glioma.

INTRODUCTION

Adult-type diffuse gliomas are the most frequent invasive primary central nervous system (CNS) tumor and is associated with a high fatality rate [1]. According to the fifth edition of WHO Central Nervous System Tumor Classification (CNS5 WHO), adult-type diffuse gliomas are divided into three categories: glioblastoma, IDH wild type (grade 4); Oligodendroglioma, IDH mutant, *1p/19q* co-deletion, (grade 2 and 3); Astrocytoma, IDH mutant (grade 2, 3 and 4) [2]. Surgery, radiotherapy and chemotherapy are the primary treatment strategies against glioma, and have achieved only limited improvements in patient prognosis [3]. In CNS5 WHO, some tumor molecular features (such as IDH1/2 mutation, TERT promoter mutation, EGFR amplification, H3 mutation, +7/-10, *1p/19q*-codeletion, *CDKN2A/B* homozygous deletion, etc..) that significantly impact on the prognosis of glioma have been further integrated and directly included in the diagnosis [4]. Nevertheless, it is still necessary to discover novel markers of glioma to improve diagnosis and predict prognosis with greater accuracy.

GPR37 is a member of G-protein-coupled receptors (GPCRs), also known as Parkinson's related endothelin like receptor (Pael-R). It is highly expressed in the brain and is related to neurological diseases such as Parkinson's disease and autism [5]. Knocking down *GPR37* in lung adenocarcinoma (LUAD) cells inhibited the malignant behavior [6], whereas elevated *GPR37* in gastric cancer cells is linked to peritoneal metastases and poor prognosis [7]. In addition, Wang et al. and Huang et al. established *GPR37* as a potential prognostic biomarker for lung adenocarcinoma and human multiple myeloma [8, 9]. Up-regulation of *GPR37* in the U251 glioma cell line accelerated cell cycle progression, activate AKT pathway and promote proliferation [10]. However, there is little conclusive data regarding the involvement of *GPR37* in the genesis and progression of glioma.

To that end, we investigated the prognostic significance and putative biological functions of *GPR37* in glioma using bioinformatics.

MATERIALS AND METHODS

Expression analysis and survival analysis of *GPR37*

Data from GEPIA2 (<http://gepia2.cancer-pku.cn/#index>) was used to validate *GPR37* mRNA expression levels in cancer and normal tissues [11]. The differential expression of *GPR37* between the glioma and normal tissues was analyzed by combining data from the GTEx (<http://commonfund.nih.gov/GTEx>) and The Cancer Genome Atlas (TCGA) (<https://portal.gdc.cancer.gov/repository>), which had been uniformly processed by the Toil process in UCSC Xena (<https://xenabrowser.net/datapages/>) [12–14]. Data-sets of glioma patients, including both genetic and clinical information, were retrieved from TCGA database and plotted using the R ggplot2 (version: 3.6.3) package.

Kaplan-Meier curves for the overall survival (OS) were plotted based on TCGA data, and compared using Cox regression. The R survival (version: 3.2-10) and survminer (version: 0.4.9) packages were used for statistical analysis and visualization.

Immunohistochemical data of *GPR37* the protein expression and distribution were analyzed in the HPA database (<https://www.proteinatlas.org/>) [15].

Patients and sample

Specimens of tumor and adjacent tissues were collected from 38 patients in the Second Affiliated Hospital of Guangzhou Medical University, who had undergone curative surgery from 2020 to 2022 in our hospital, which was approved by Institutional Ethics Committee in the Second Affiliated Hospital of Guangzhou Medical University. 38 patients' tumor tissues were used for immunohistochemistry. Written informed consents were acquired from each patient relying on guidelines of the Declaration of Helsinki.

Immunohistochemistry (IHC)

Tissue sections were deparaffinised, soaked in TrisEDTA buffer (pH 9.0) boiled in a microwave and

then incubated with antibodies against *GPR37* (1:250; ab218134, Abcam) at 4°C for 12 h. The next day, slides were washed, stained with secondary antibodies and 3, 3'-diaminobenzidine, counterstained with hematoxylin, dehydrated and mounted. The sections were reviewed and scored independently by two observers. The results of immunohistochemistry of *GPR37* between the different glioma was analyzed by Image Pro Plus image analysis software [16], take the average optical density (AOD) as the measurement index and plotted using the R ggplot2 (version: 3.6.3) package [17].

Univariate and multivariate cox regression analysis

TCGA data were combined and plotted in a matrix. The impact of *GPR37* expression and other clinicopathological parameters (grade, histological type, *CDKN2A/B* homozygous deletion, age, gender and primary therapy outcome) on the OS and DSS was evaluated using univariate and multivariate cox analysis, with *P* value < 0.05 as the cut-off criterion. The R package 'forestplot,' was used to calculate the *P* value, HR and 95% CI of each variable.

Gene set enrichment analysis and co-expressed genes

The gene co-expressed with *GPR37* were obtained using the LinkFinder module of LinkedOmics (<http://www.linkedomics.org/>), and a heat map of the top 50 positively or negatively correlated genes was generated [18]. The genes and proteins that physically interact with *GPR37* were identified using the STRING database (<https://string-db.org>) [19], and a protein-protein interaction (PPI) network was built with a total score of > 0.7 (high confidence) and visualized using Cytoscape [20]. The glioma samples of TCGA database were then separated into the *GPR37*^{high} and *GPR37*^{low} groups, and the differentially expressed genes (DEGs) between the groups were identified using the DESeq2 R (version: 1.26.0) package with *P* < 0.05 and |log FC| ≥ 1.0 as the thresholds [21]. The hub genes were functionally annotated using Gene Ontology (GO) keywords (biological process, cellular component and molecular function categories) and Kyoto Encyclopedia of Genes and Genomes (KEGG) pathways [22, 23].

The ClusterProfiler program was used to perform gene set enrichment analysis (GSEA) to identify biological pathways that differed significantly between the *GPR37*^{high} and *GPR37*^{low} groups [24, 25]. Studies were run in the MSigDB database (<https://www.gsea-msigdb.org/gsea/msigdb/collections.jsp#C2>) with a number of size 3 and 10000 simulations [26]. Genes with false discovery rate (FDR) < 0.25 and *p*_{adjust} < 0.05 were considered statistically significant.

Tumor infiltration analysis

The single-sample GSEA (ssGSEA) was used to quantify the tumor infiltration of 24 immune cell types based on TCGA data using the R GSVA package [27, 28]. The gene panels for each immune cell type were selected as per a recent report. The correlation of *GPR37* expression with the infiltration of eosinophils, macrophages, NK cells, neutrophils and T cells was analyzed. OS was examined as a function of *GPR37* expression, M2 macrophage and cancer-associated fibroblasts (CAFs) in the TIMER2.0 (<http://timer.cistrome.org>) database [29].

DNA methylation analysis

The relationship between DNA methylation and *GPR37* expression was investigated using Pearson correlation analysis. Correlation coefficients (R) and Benjamin-Hochberg-adjusted *P*-values for different methylation sites were obtained. *GPR37* methylation and the Kaplan-Meier-based correlation between *GPR37* hyper/hypomethylation and OS were visualized using the MethSurv (<https://biit.cs.ut.ee/methsurv>) program [30].

Availability of data and materials

All of the data utilized in this study came from publicly accessible databases. The databases that were used throughout the investigation are listed below. Gene Expression Profiling Interactive Analysis 2 database (GEPiA2, <http://gepia2.cancer-pku.cn/#index>), Genotype-Tissue Expression Project (GTEx, <http://commonfund.nih.gov/GTEx>), The Cancer Genome Atlas (TCGA, <https://portal.gdc.cancer.gov/repository>), XENA platform (UCSC Xena, <https://xenabrowser.net/datapages/>), Human Protein Atlas (<https://www.proteinatlas.org/>), LinkedOmics database (<http://www.linkedomics.org/>), STRING database (<https://string-db.org>), Molecular Signatures database (MSigDB, <https://www.gsea-msigdb.org/gsea/msigdb/collections.jsp#C2>), Tumor Immune Estimation Resource 2.0 database (TIMER2.0, <http://timer.cistrome.org>), MethSurv database (<https://biit.cs.ut.ee/methsurv>).

RESULTS

GPR37 is overexpressed in glioma and associated with clinicopathological factors

The flow chart of the study is shown in Figure 1. The classification of histological type and grade of all glioma samples (listed in Supplementary Table 1) are consistent with the recommendations of CNS5 WHO

[31]. *GPR37* expression levels were analyzed in pan-tumor tissues and their normal counterparts (Figure 2A). As shown in Figure 2B, *GPR37* was significantly up-regulated in glioma compared to normal brain tissues (Figure 2B). Furthermore, *GPR37* expression was higher in CNS WHO grade 4 tumors relative to the CNS WHO grade 2 & 3 tumors (Figure 2C). Consistent with

this, overexpression of *GPR37* was linked to poor prognosis in glioma patients in terms of the likelihood of overall survival (OS) (Figure 2D, $P < 0.001$). In addition, immunohistochemical analysis was applied to observe the distribution and protein levels of *GPR37*. The clinicopathological characteristics of 38 patients are shown in Supplementary Table 2. With normal tissues

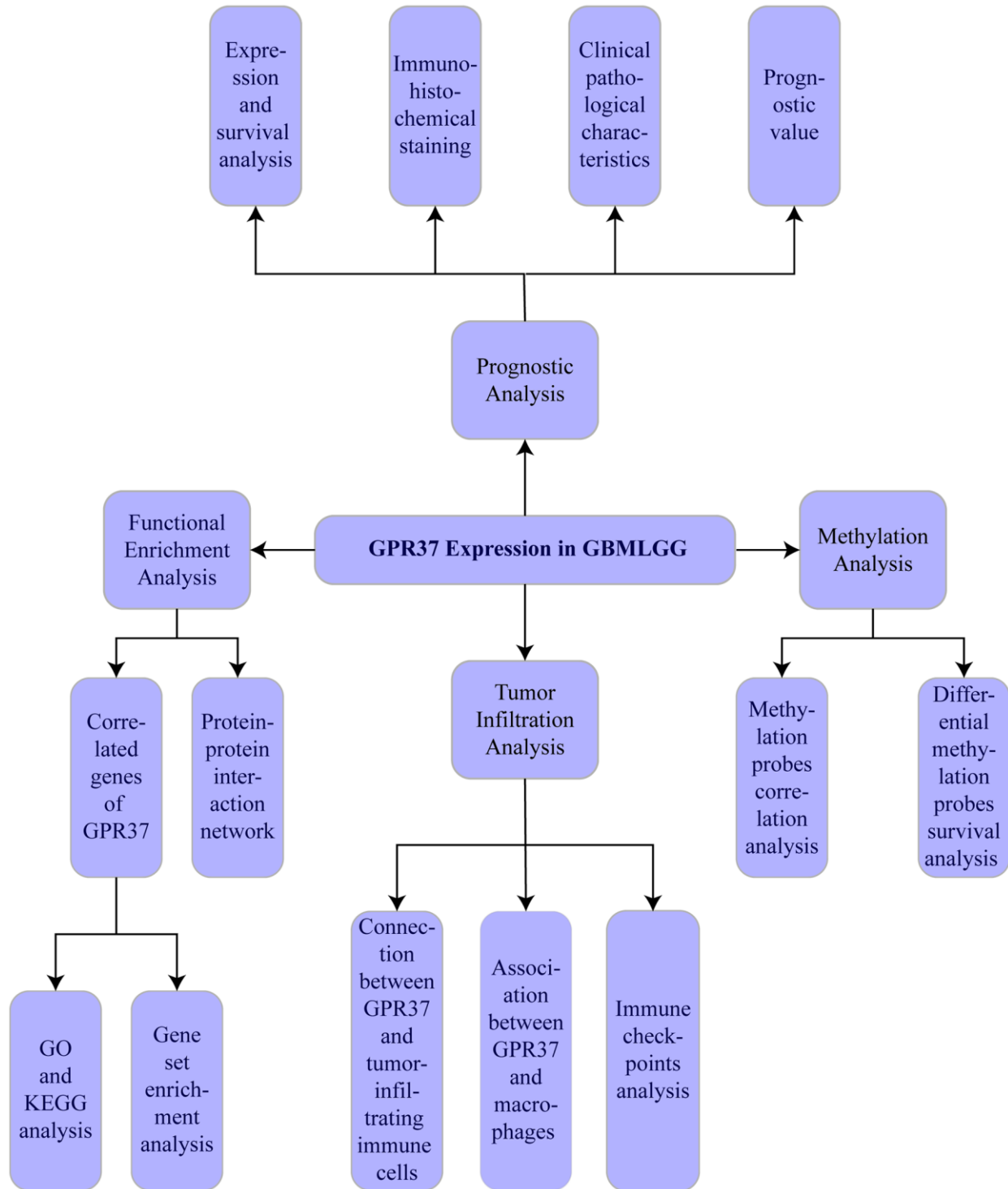


Figure 1. Flow chart of the study.

adjacent to the tumor as the control group, the *GPR37* expression in different grade of glioma were statistically analyzed in 38 samples. As shown in Figure 3A–3C, *GPR37* was expressed in neurons and glia and exhibited more elevated expression levels in GBM tissues. Immunohistochemical staining of clinical 38 samples also confirmed that the different level of *GPR37* expression in tumor tissues were in CNS WHO grade 2, 3 and 4 of glioma (Figure 3D, 3E).

We further analyzed the data from TCGA databases to explore a possible link between *GPR37* and clinicopathological characteristics of glioma patients.

The patients were divided into *GPR37*^{high} ($n = 353$) and *GPR37*^{low} ($n = 352$) groups based on the median expression value. As shown in Table 1, elevated *GPR37* in glioma was significantly associated with the CNS WHO grade, histological type, *1p/19q* codeletion, the IDH status, *CDKN2A/B* homozygous deletion, age and primary therapy outcome ($P < 0.05$), while no significant correlation was seen with gender ($P > 0.05$). Moreover, univariate logistic regression analysis (Table 2) showed a significant correlation of *GPR37* mRNA expression with CNS WHO grade (G4 vs. G2 & G3, OR = 0.380, 95% CI (0.069–0.692), $P < 0.001$), histological type (Glioblastoma, IDH

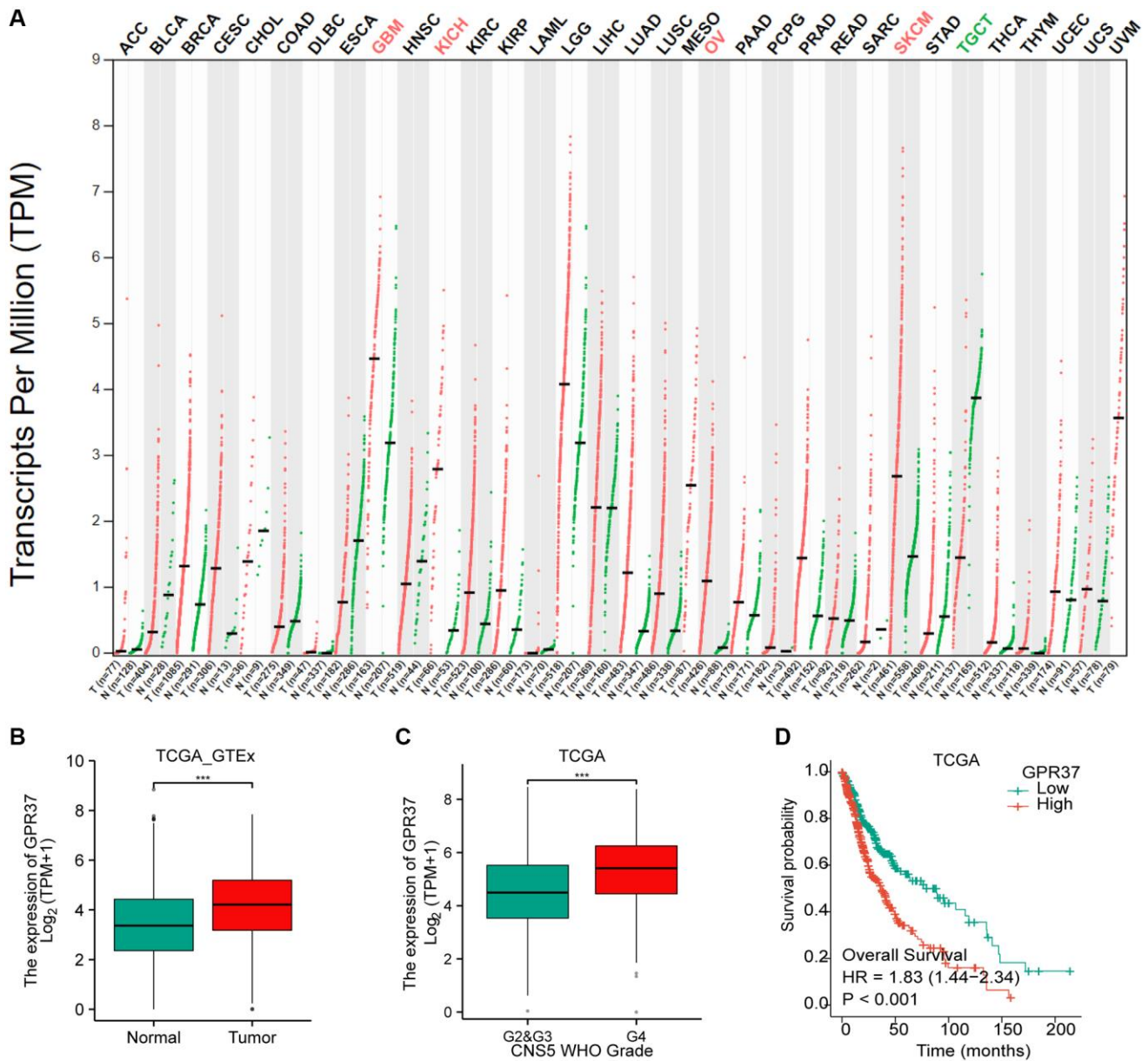


Figure 2. Differential *GPR37* expression in glioma and prognostic relevance. (A) Pan-cancer *GPR37* mRNA levels. (B) *GPR37* expression across glioma samples and normal tissues. (C) Survival curves of *GPR37*^{high} and *GPR37*^{low} glioma patients in TCGA dataset (C, D). Abbreviations: OS: overall survival; LGG: low grade glioma.

wildtype vs. Oligodendroglioma, IDH mutation, *1p/19q*-code1 vs. Astrocytoma, IDH mutation, OR = 0.397, 95% CI (0.040–0.754), $P < 0.001$, *CDKN2A/B* homozygous deletion (non-homdel vs. homdel, OR = 1.865, 95% CI (1.495–2.234), $P < 0.001$), age (≤ 60 vs. > 60 , OR = 1.466, 95% CI (1.095–1.836), $P < 0.001$).

***GPR37* expression is an independent prognostic factor in glioma**

Univariate Cox regression analysis of *GPR37* expression, grade, histological type, *CDKN2A/B* homozygous deletion, age, gender and primary therapy

outcome using TCGA data indicated that *GPR37* was significantly correlated with both OS (HR 1.851, 95% CI = 1.450, 2.362, $p < 0.001$) and DSS (HR 2.031, 95% CI = 1.565, 2.637, $p < 0.001$). In addition, multivariate analysis identified *GPR37* as an independent risk factor for OS (HR 1.771, 95% CI = 1.180, 2.658, $p = 0.006$) and DSS (HR 1.834, 95% CI = 1.196, 2.813, $p = 0.005$, Supplementary Tables 3 and 4). Figure 4 shows a summary of the findings.

Co-expressed genes of *GPR37* and GSEA

To explore the role played by *GPR37* in the development and progression of glioma, we screened

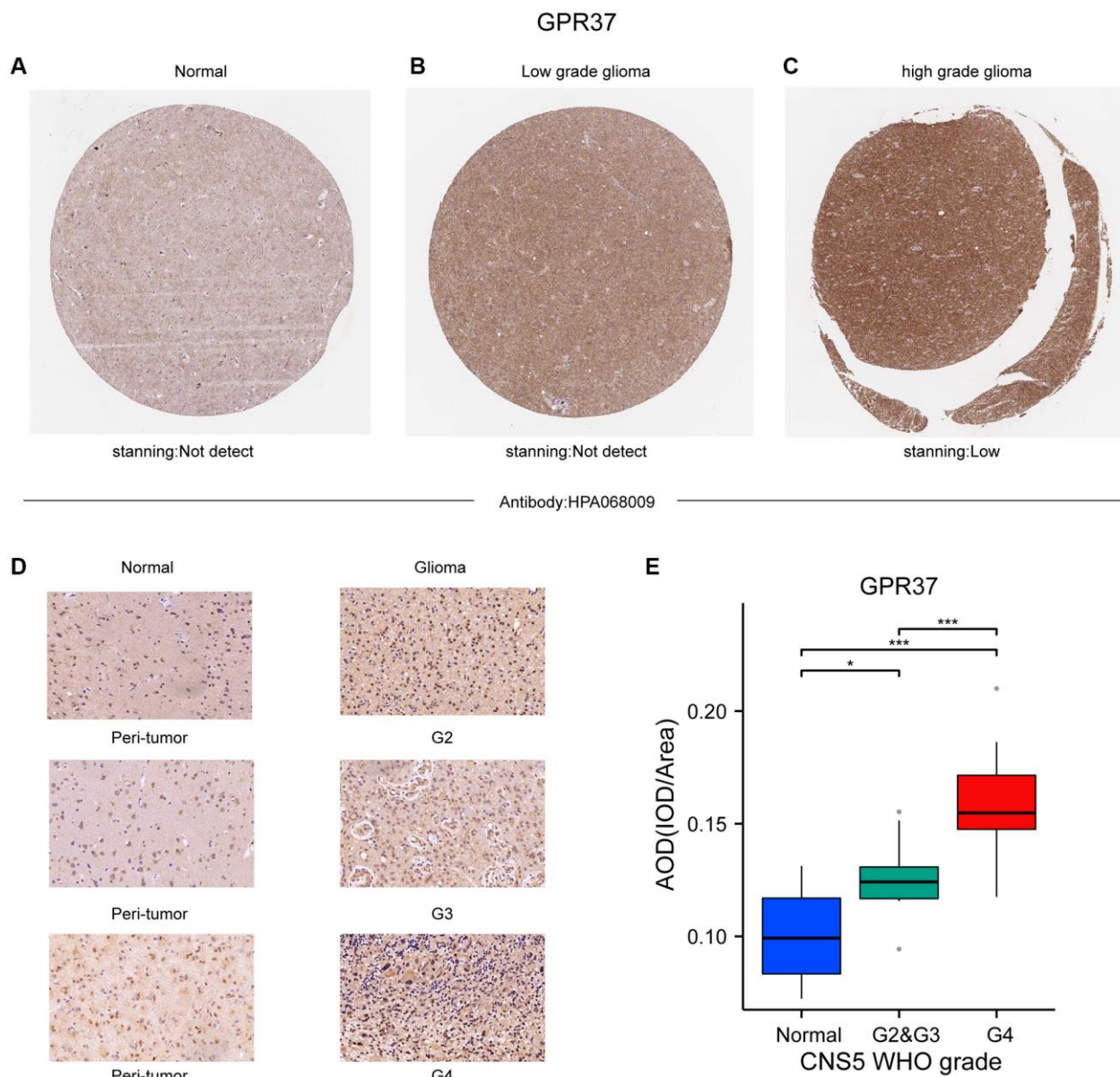


Figure 3. (A–C) Representative IHC images from the Human Protein Atlas showing *in situ* *GPR37* protein expression in glioma tissues. (D, E) *GPR37* expression in different grades of glioma was statistically analyzed in 38 gliomas using normal tissues adjacent to the tumor as the control group.

Table 1. GPR37 mRNA expression and clinicopathological variables of glioma.

Characteristics	Low expression of GPR37	High expression of GPR37	P value
<i>n</i>	353	352	
Grade, <i>n</i> (%)			
G4	103 (14.8%)	182 (26.1%)	<0.001
G2 & G3	247 (35.4%)	166 (23.8%)	
Histology, <i>n</i> (%)			
Glioblastoma, IDH WT	81 (11.7%)	166 (24%)	<0.001
Oligodendroglioma, IDH mut, <i>1p/19q</i> codel	115 (16.6%)	57 (8.2%)	
Astrocyoma, IDH mut	150 (21.7%)	122 (17.7%)	
<i>CDKN2A/B</i> homozygous deletion, <i>n</i> (%)			
Non-homdel	296 (42%)	259 (36.7%)	<0.001
Homdel	57 (8.1%)	93 (13.2%)	
IDH, <i>n</i> (%)			
WT	81 (11.7%)	166 (24%)	<0.001
Mutant	265 (38.4%)	179 (25.9%)	
<i>1p/19q</i> , <i>n</i> (%)			
Non-codel	233 (33.6%)	289 (41.6%)	<0.001
Codel	115 (16.6%)	57 (8.2%)	
Gender, <i>n</i> (%)			
Male	202 (28.9%)	199 (28.5%)	0.922
Female	149 (21.3%)	149 (21.3%)	
Age, <i>n</i> (%)			
≤60	290 (41.5%)	266 (38.1%)	0.043
>60	61 (8.7%)	82 (11.7%)	
Primary therapy outcom, <i>n</i> (%)			
CR	67 (14.4%)	73 (15.7%)	0.037
SD	81 (17.4%)	67 (14.4%)	
PD	51 (11%)	61 (13.1%)	
PR	43 (9.2%)	22 (4.7%)	

Table 2. GPR37 expression correlated with clinicopathological characteristics.

Characteristics	Total (N)	Odds Ratio (95% CI)	P value
CNS WHO grade (G4 vs. G2 & G3)	698		
G4	285	Reference	<0.001
G2 & G3	413	0.380 (0.069–0.692)	
Histological Type	691		
Glioblastoma, IDH wildtype	247	Reference	<0.001
Oligodendroglioma, IDH mutation, <i>1p/19q</i> -codel	172	0.242 (–0.172–0.656)	
Astrocyoma, IDH mutation	272	0.397 (0.040–0.754)	
<i>CDKN2A/B</i> homozygous deletion	705		
Non-homdel	555	Reference	<0.001
Homdel	150	1.865 (1.495–2.234)	
Age	699		
≤60	556	Reference	0.043
>60	143	1.466 (1.095–1.836)	

Gender	699		
Male	401	Reference	
Female	298	1.015 (0.715–1.315)	0.922
Primary therapy outcome	465		
PR & CR	205	Reference	
PD & SD	260	1.123 (0.756–1.490)	0.536

for the co-expressed genes using the LinkedOmics database. The heatmaps of the top 50 positively and negatively *GPR37*-linked genes are shown in Supplementary Figure 1A, 1B. A PPI network of *GPR37* was constructed, and the top ten hub genes were *PARK2*, *UBE2G2*, *UBE2G1*, *SEPT5*, *SNCAIP*, *PSAP*, *GRP*, *GABARAPL2*, *HSPA4* and *SYVN1* (Figure 5A).

GO enrichment analysis further showed that the hub genes were significantly associated with sensory perception of mechanical stimulus, axon ensheathment, ensheathment of neurons, ciliary movement and other BP terms, whereas apical part of cell, apical plasma membrane, cilium plasm, axoneme etc., were the enriched CC terms, and passive transmembrane

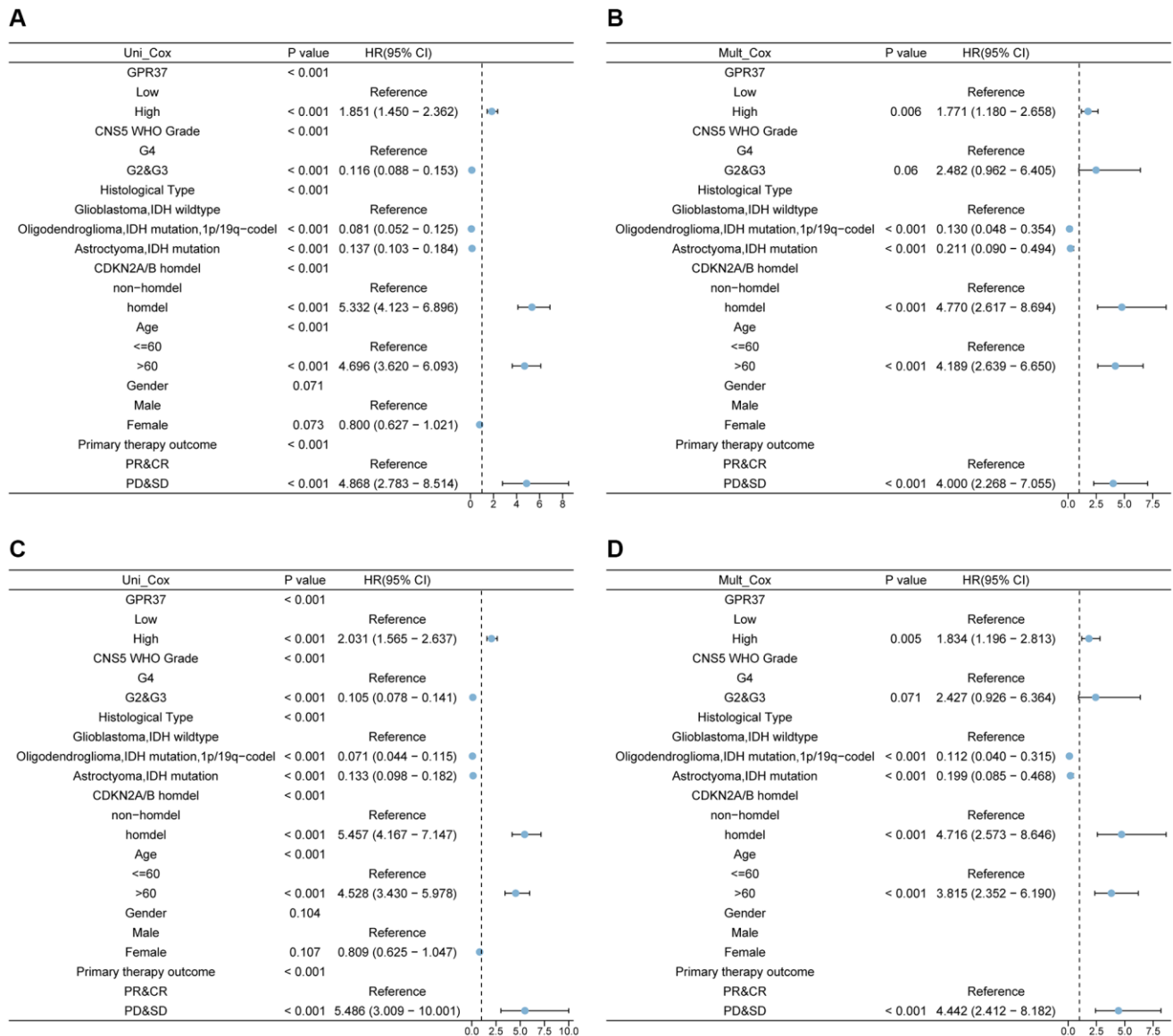


Figure 4. Univariate and multivariate Cox analysis of *GPR37* expression, grade, histological type, *CDKN2A/B* homozygous deletion (homdel), radiation therapy, age, and gender for OS (A, B) and DSS (C, D). Abbreviations: OS: overall survival; DSS: disease specific survival; HR: hazard ratio.

transporter activity, channel activity, substrate-specific channel activity etc., were the enriched MF terms. In addition, KEGG analysis revealed a significant association with ether lipid metabolism, fat digestion and absorption, and histidine metabolism pathways (Figure 5B–5E).

GSEA was used to discriminate between the *GPR37*^{high} and *GPR37*^{low} glioma populations (adjust *P* value < 0.05, FDR < 0.05). The *GPR37*^{high} phenotype a significant enrichment of GO terms for positive regulation of macrophage derived foam cell differentiation, negative regulation of T cell receptor signaling pathway,

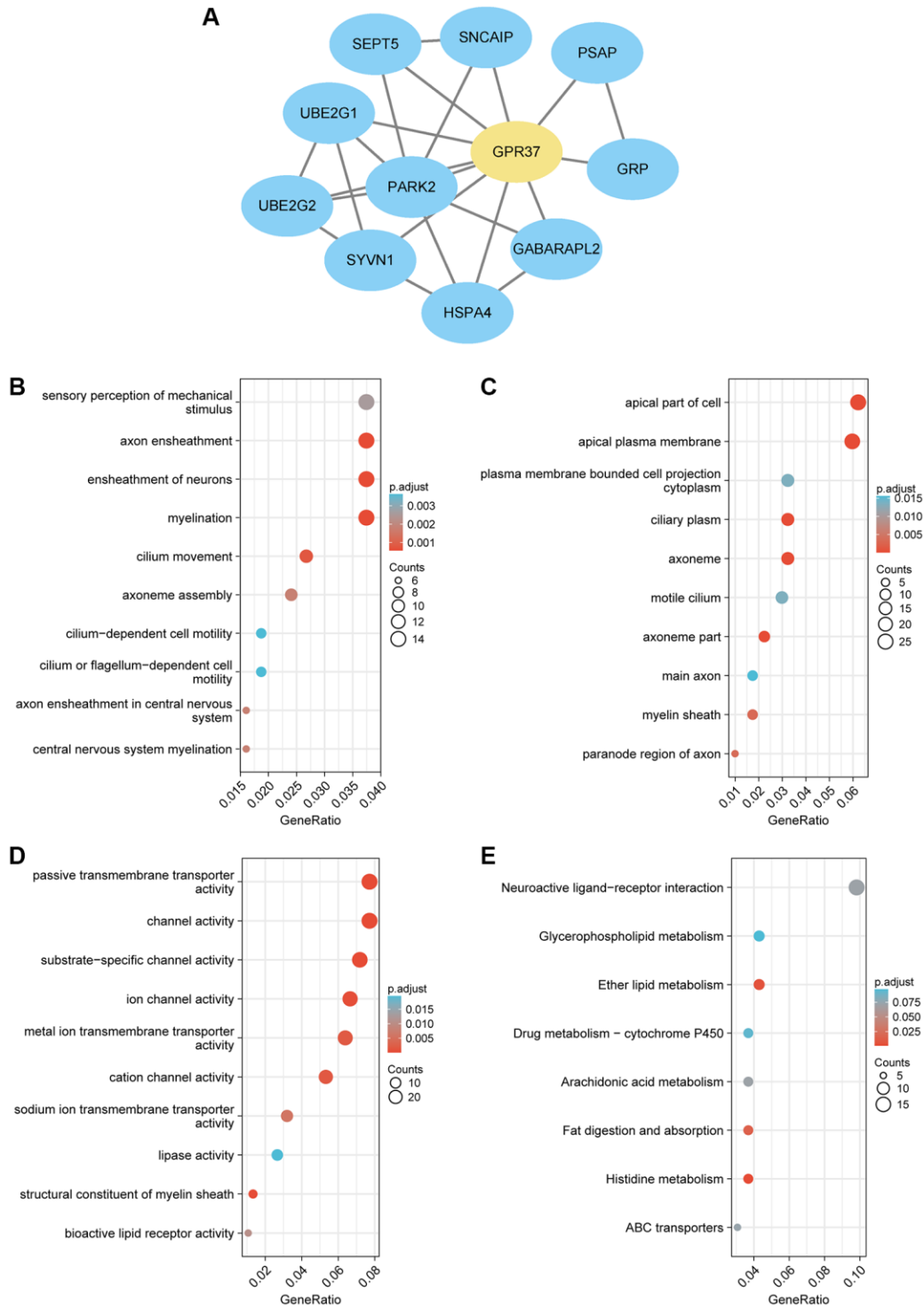


Figure 5. (A) PPI network of *GPR37*-related genes in glioma. (B–E) Gene set enrichment analysis based on GO analysis including BP, CC and MF terms, and KEGG pathway analysis for all linked hub genes of *GPR37* in glioma.

leukocyte proliferation, B cell proliferation and myeloid leukocyte differentiation, whereas immunoglobulin complex, immunoglobulin complex circulating, antigen binding, immunoglobulin receptor binding and humoral immune response mediated by circulating

immunoglobulin were significantly enriched in the *GPR37*^{low} phenotype (Figure 6A). Neuroactive ligand receptor interaction, calcium signaling pathway, B cell receptor signaling pathway, PPAR signaling pathway, and toll like receptor signaling pathway were

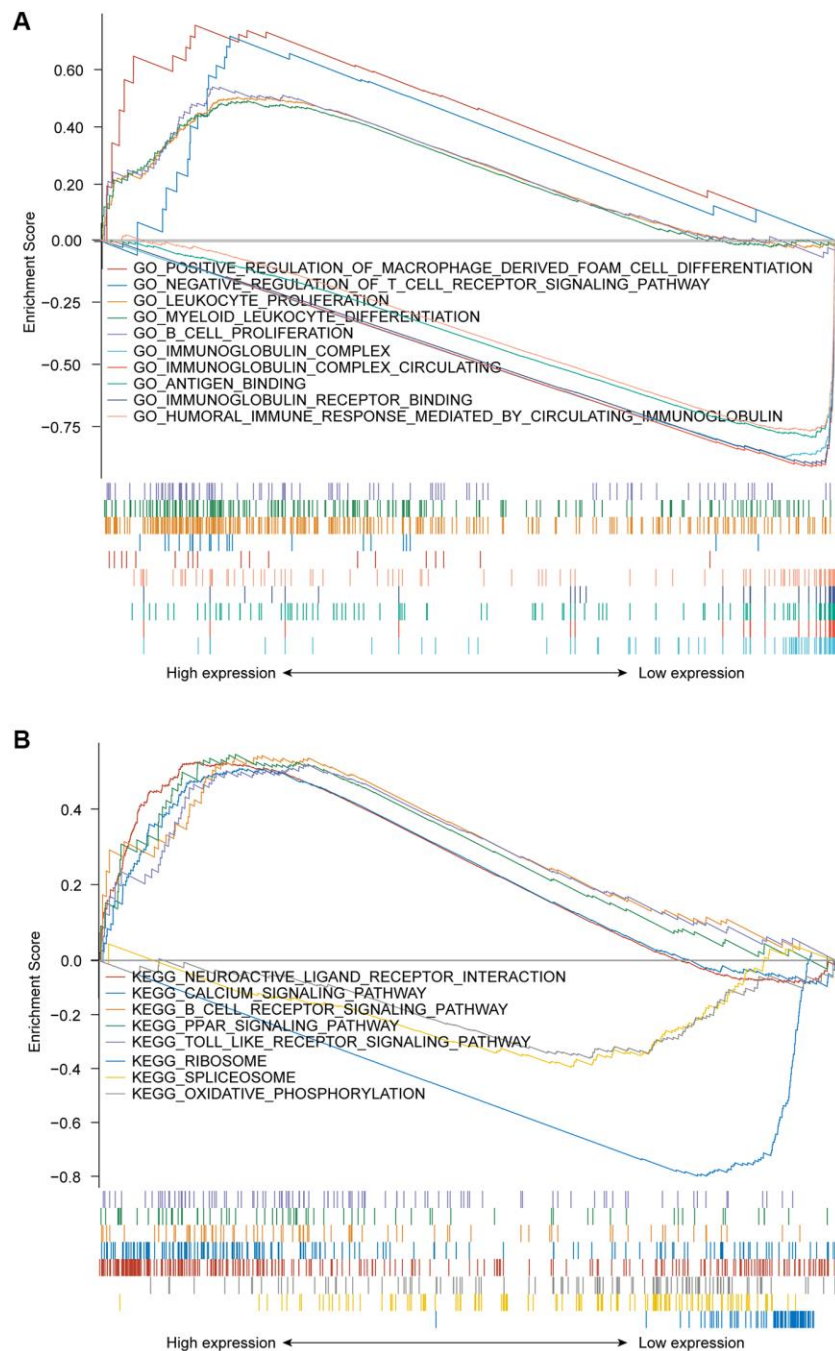


Figure 6. (A) GSEA results showing differential enrichment of GO terms as a function of *GPR37* expression. Top 5 GO terms for *GPR37*^{high}-positive regulation of macrophage derived foam cell differentiation, negative regulation of T cell receptor signaling pathway, leukocyte proliferation, B cell proliferation and myeloid leukocyte differentiation. Top 5 GO terms for *GPR37*^{low}- immunoglobulin complex, immunoglobulin complex circulating, antigen binding, immunoglobulin receptor binding and humoral immune response mediated by circulating immunoglobulin. **(B)** GSEA results showing differential enrichment of KEGG pathways as a function of *GPR37*. Top 5 KEGG pathways for *GPR37*^{high}-neuroactive ligand receptor interaction, calcium signaling pathway, B cell receptor signaling pathway, PPAR signaling pathway and toll like receptor signaling pathway. Two KEGG pathways in *GPR37*^{low}- ribosome, spliceosome and oxidative phosphorylation. All results of GSEA were based on NES, adjusted *P* value and FDR value. GSEA, gene set enrichment analysis.

the top 5 KEGG pathways in the *GPR37*^{high} groups, whereas the *GPR37*^{low} phenotype was associated with ribosome, spliceosome and oxidative phosphorylation pathways (Figure 6B). The GO and KEGG components are summarized in Supplementary Table 5. These results indicated that *GPR37* is involved in the development and progression of glioma.

Tumor infiltration analysis

Tumor-infiltrating lymphocytes are reliable indicators of cancer survival. Therefore, we also analyzed the correlation between *GPR37* expression in glioma and immune infiltration. As shown in Figure 7A, *GPR37* expression correlated significantly with the infiltration

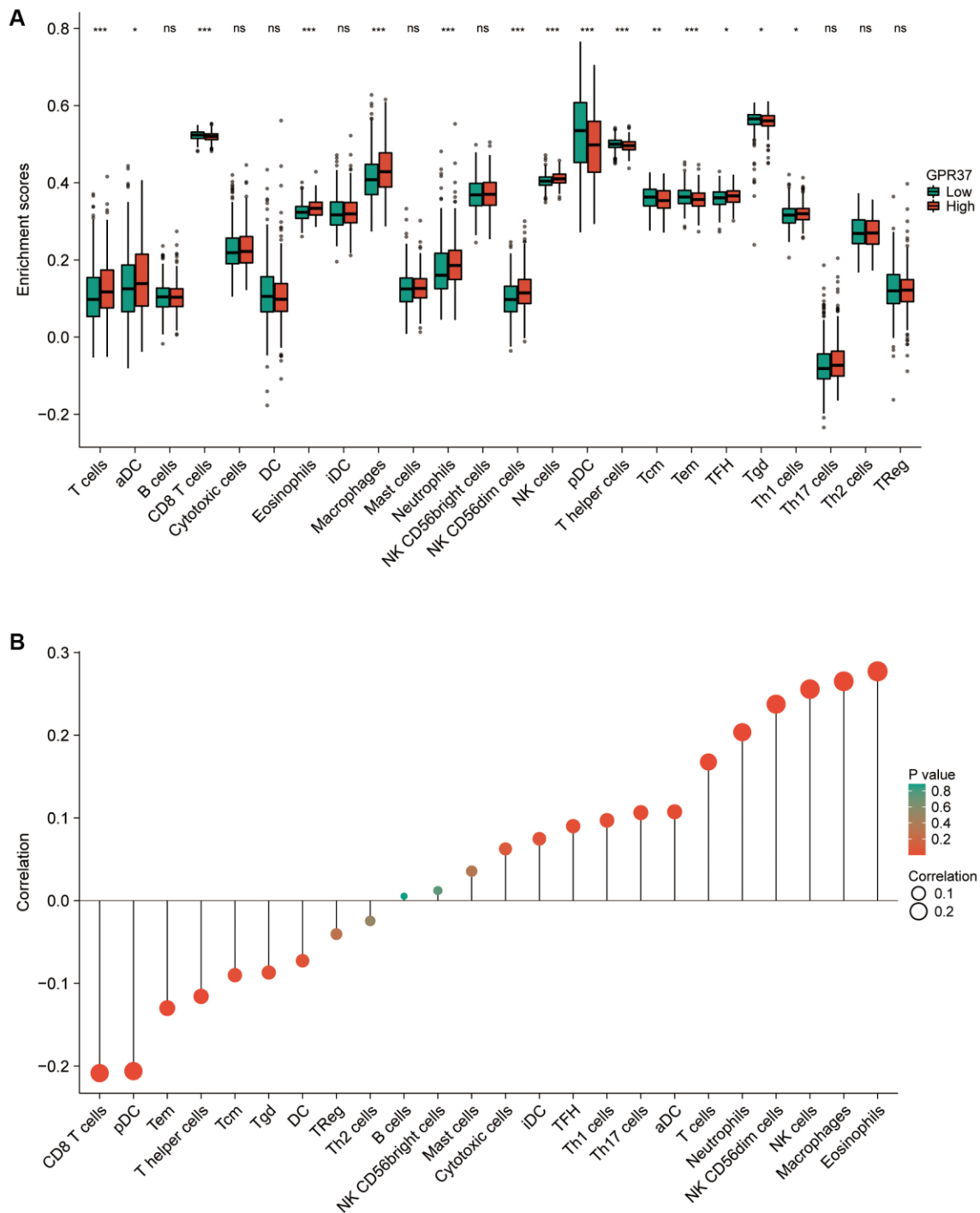


Figure 7. (A) Correlation between *GPR37* expression and 24 tumor-infiltrating immune cell types. **(B)** Eosinophils, Macrophages, NK cells, Neutrophils and T cells were positively connected with *GPR37* expression, while CD8 T cells, pDCs, Tem, T helper cells, Tcm, and Tgd were negatively correlated. ns, $p \geq 0.05$; * $p < 0.05$; ** $p < 0.01$; *** $p < 0.001$.

of T cells, CD8 T cells, eosinophils, macrophages, neutrophils, NK CD56^{dim} cells, NK cells, plasmacytoid DCs (pDCs), T helper cells, T effector memory (Tem) cells ($P < 0.001$), T central memory (Tcm) cells ($P < 0.01$), T follicular helper (Tfh) cells, tgD, Th1 cells and activated DCs (aDCs) ($P < 0.05$). On the other hand, no significant correlation was seen with B cells,

cytotoxic cells, DCs, immature DCs (iDCs), mast cells, NK CD56^{bright} cells, Th17 cells, Th2 cells and Treg cells. As shown in Figure 7B, *GPR37* was positively associated with infiltration levels of Eosinophils ($r = 0.277$, $P < 0.001$, Figure 8A), Macrophages ($r = 0.265$, $P < 0.001$, Figure 8A), NK cells ($r = 0.256$, $P < 0.001$, Figure 8A), NK CD56^{dim} cells ($r = 0.251$,

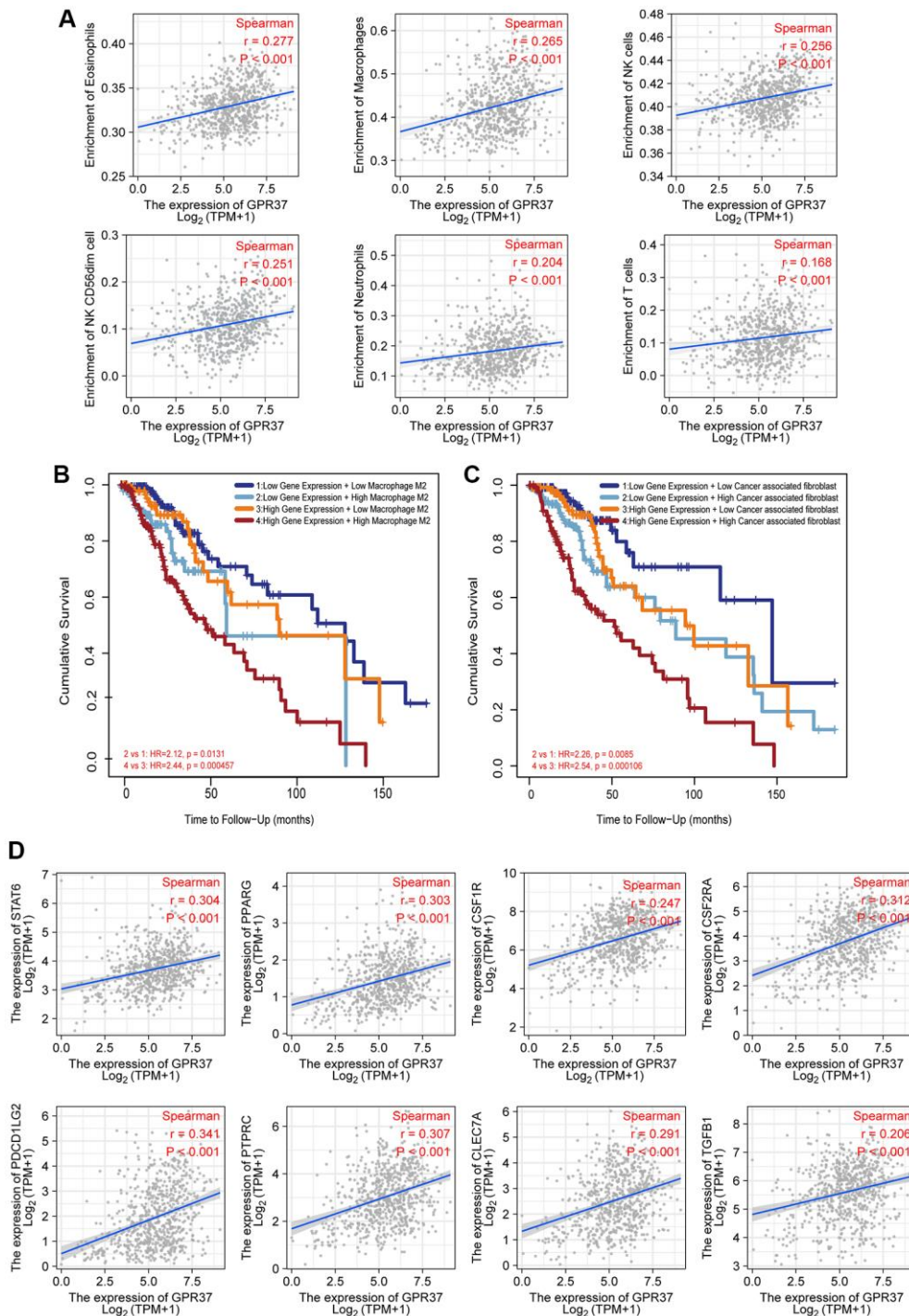


Figure 8. Correlation between immunological infiltrates and *GPR37* expression. (A) Eosinophils, Macrophages, NK cells, NK CD56^{dim} cells, Neutrophils, and T cells were all positively linked with *GPR37* expression. (B, C) Infiltration of M2 macrophages and cancer-associated fibroblasts were associated with poor outcome. (D) The M2 markers were positively linked with *GPR37* expression.

$P < 0.001$, Figure 8A), Neutrophils ($r = 0.204$, $P < 0.001$, Figure 8A), T cells ($r = 0.168$, $P < 0.001$, Figure 8A), and negatively with that of CD8 T cells, pDC, Tem, T Helper cells, Tcm, Tgd etc. Furthermore, high M2 macrophage infiltration along with high expression of *GPR37* portended poor prognosis (Figure 8B, HR = 2.44, $p = 0.000457$), as did higher infiltration of cancer associated fibroblasts (Figure 8C). In addition, the expression levels of most M2 macrophage markers, including *STAT6*, *PPARG*, *CSF1R*, *CSF2RA*, *PDCD1LG2*, *PTPRC*, *CLEC7A*, and *TGF-1*, were positively correlated with *GPR37* (Figure 8D). Thus, *GPR37* may influence macrophage polarization in glioma.

Correlation between immune checkpoints and *GPR37* expression

We examined the relationship between *GPR37* levels and those of common immune checkpoints (ICPs) to determine the possible impact of *GPR37* expression on the response to immunotherapy. The *GPR37*^{high} group had high levels of *CD274*, *PDCD1LG2*, *PDCD1*, *CD80*, *CD86*, *CD28*, *CTLA4*, *PVR*, *TIGIT*, *CD96*, *CD226*, *HAVCR2*, *LGALS9*, *CD47*, *SIPRA*, *CD200*, *CD200R1*, *CIITA*, and *LAG3* expression (Figure 9A). Furthermore, TCGA-based analyses revealed a positive relationship between *GPR37* expression and *CD274*, *PDCD1LG2*, *PDCD1*, *CD80*, *CD86*, *CTLA4*, *PVR*, *TIGIT*, *CD96*, *CD226*, *HAVCR2*, *LGALS9*, *CD47*, *SIPRA*, *CD200*, *CD200R1*, *CIITA*, and *LAG3* expression (Figure 9B–9Q). These higher ICP levels suggested that patients with strong *GPR37* expression would have a better immunotherapy response.

GPR37 DNA methylation analysis

Since DNA methylation is a critical epigenetic modification that is associated with tumor progression, we also screened for the methylated sites in *GPR37* and analyzed the correlation between *GPR37* methylation and expression in glioma. As shown in Figure 10A, 10B, there was a significant negative correlation between the extent of DNA methylation in *GPR37* and its expression levels in LGG, and to a lesser extent in GBM. In addition, hypomethylation at cg02960853, cg26141626, cg01667837, cg14311320, cg16847696, cg17152484, cg22230167, cg23428445, cg09458673, cg07392724, cg17052813, cg10503827, cg06592333, cg27533119, cg23799901, cg07376282 and cg26278103 in the *GPR37* promoter was linked to poor prognosis (Figure 10C–10U). These findings were in line with our earlier study.

DISCUSSION

GPCRs are the largest family of cell surface proteins involved in signal transduction, and key participants in

tumor growth and metastasis [32]. Aberrant expression and function of GPCRs in tumor cells have been linked to autonomous proliferation, immune escape, increased metabolism, and invasion and metastasis to other tissues [33]. Although the involvement of *GPR37* in the growth and prognosis of several malignancies has been partially validated, its role in glioma remains unknown [34–36]. Through bioinformatics analysis, we found that *GPR37* was noticeably up-regulated in glioma tissues, and associated with poor prognosis. In addition, we also identified *GPR37* as an independent prognostic factor for both OS and DSS in glioma.

PPI network analysis further revealed that *GPR37* interacts with *PARK2*, *UBE2G2*, *UBE2G1*, *SEPT5*, *SNCAIP*, *PSAP*, *GRP*, *GABARAPL2*, *HSPA4* and *SYVNI*, which have been linked to tumor development in previous studies [37–44]. *GPR37* was previously identified as the receptor of Parkin, an E3 ubiquitin ligase encoded by *PARK2*, involved in ubiquitination and proteasome mediated degradation/clearance of misfolding proteins, which is closely related to tumor development [45–47]. Furthermore, one of the characteristics of *GPR37* is that it has an abnormally long N-terminal [48]. It has been proved that N-terminal truncation will make the surface transport of *GPR37* more efficient, resulting in enhanced expression of *GPR37* [49]. During the transport of *GPR37* protein from the endoplasmic reticulum (ER) to the cell membrane, metalloproteinases (MPs) can process the N-terminal of *GPR37*, so that *GPR37* can be transformed from precursor form to mature complete glycosylation form and stably exist in the cell membrane in the cleaved form [50]. In our research, GO enrichment analysis showed that *GPR37* is enriched in apical part of cell, apical plasma membrane, cilium plasm, axoneme etc., has molecular function of passive transmembrane transporter activity, channel activity, substrate-specific channel activity etc., and participates in biological processes such as sensory perception of mechanical stimulus, axon ensheathment, ensheathment of neurons, ciliary movement and so on. In addition to these, KEGG analysis revealed that *GPR37* may be involved in regulating ether lipid metabolism, fat digestion and absorption, and histidine metabolism pathways. Ether lipid biosynthesis is unique to the peroxisome and is regulated by the peroxisome proliferator activated receptor (PPAR) [51–54]. PPAR- γ is the major receptor in the central nervous system (CNS) and is generally expressed at a low level [55]. Nwankwo and Khoo et al. discovered that PPAR expression was significantly higher in gliomas compared to normal astrocytes, and was associated with a poor prognosis [56, 57]. PPAR- γ primarily regulates gene expression at the transcriptional level, and is in turn regulated by transcription factors, microRNAs and

kinases, thus affecting stemness and malignant transformation [58]. We found that the highly expressed *GPR37* was enriched in the PPAR signaling pathway, which is consistent with previous findings. In summary, *GPR37* may increase the incidence and development of

glioma by regulating the PPAR pathway, which requires more investigation.

The tumor immune microenvironment consists of various immune and inflammatory cells that play an

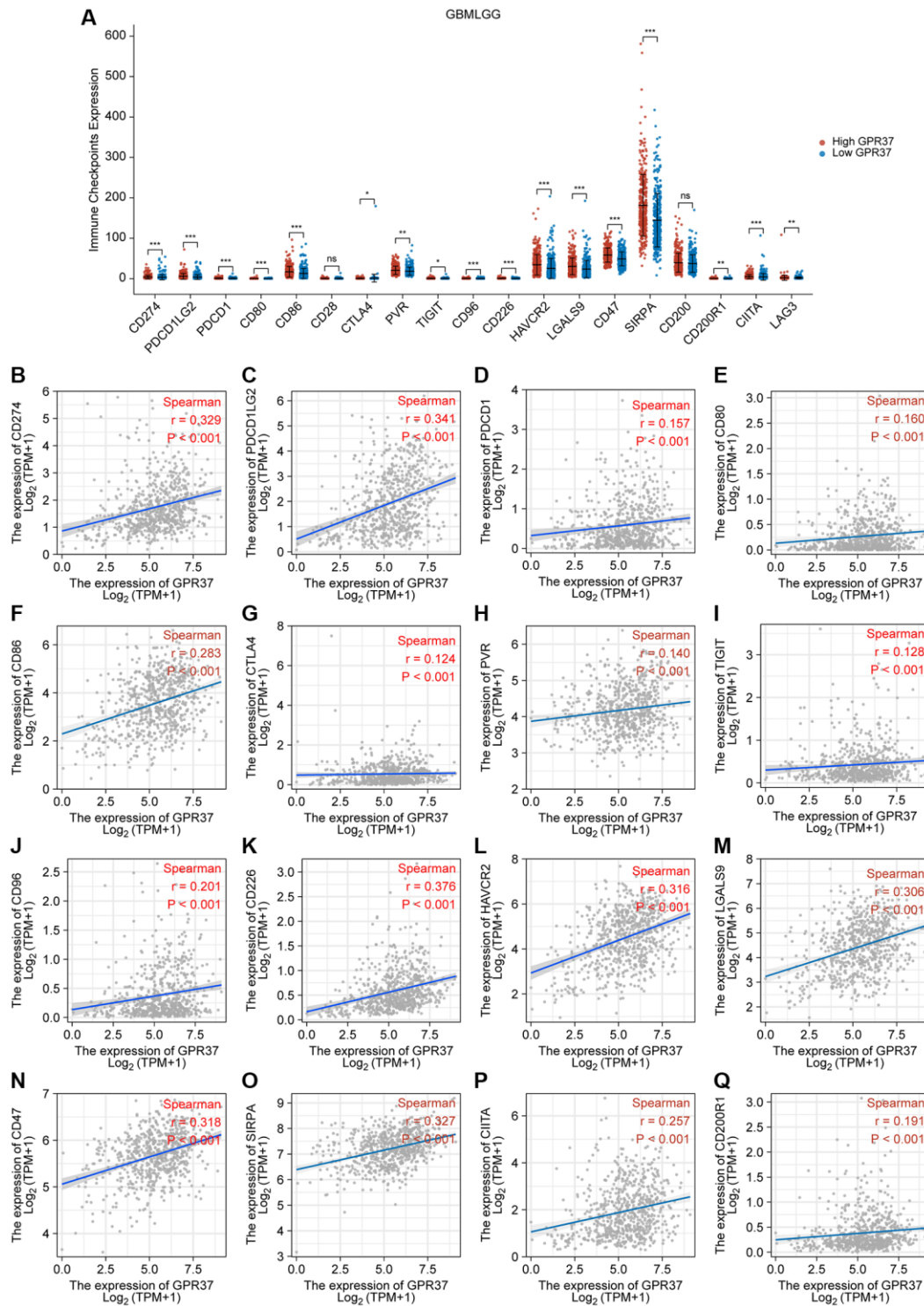


Figure 9. Correlation between *GPR37* expression levels and common immune checkpoints (ICPs). (A) Graph showing expression of ICPs in the *GPR37*^{high} (red) and *GPR37*^{low} (blue) groups. (B–Q) Spearman correlation coefficients for the association between the expression levels of *GPR37* and ICPs. **P* < 0.05, ***P* < 0.01, ****P* < 0.001.

important role in tumor development and progression [59]. In this study, we confirmed that the abnormal expression of *GPR37* is related to the increased infiltration of eosinophils, macrophages, NK CD56^{dim} cells, NK cells, neutrophils and T cells etc. A number of growth factors and cytokines can be released by tumor

associated macrophages (TAMs), which are drawn into the glioma environment, have immunological capabilities, and are able to react to the growth factors produced by cancer cells [60]. TAMs encourage tumor migration, survival, and proliferation in this way. *GPR37* was significantly associated with the infiltration

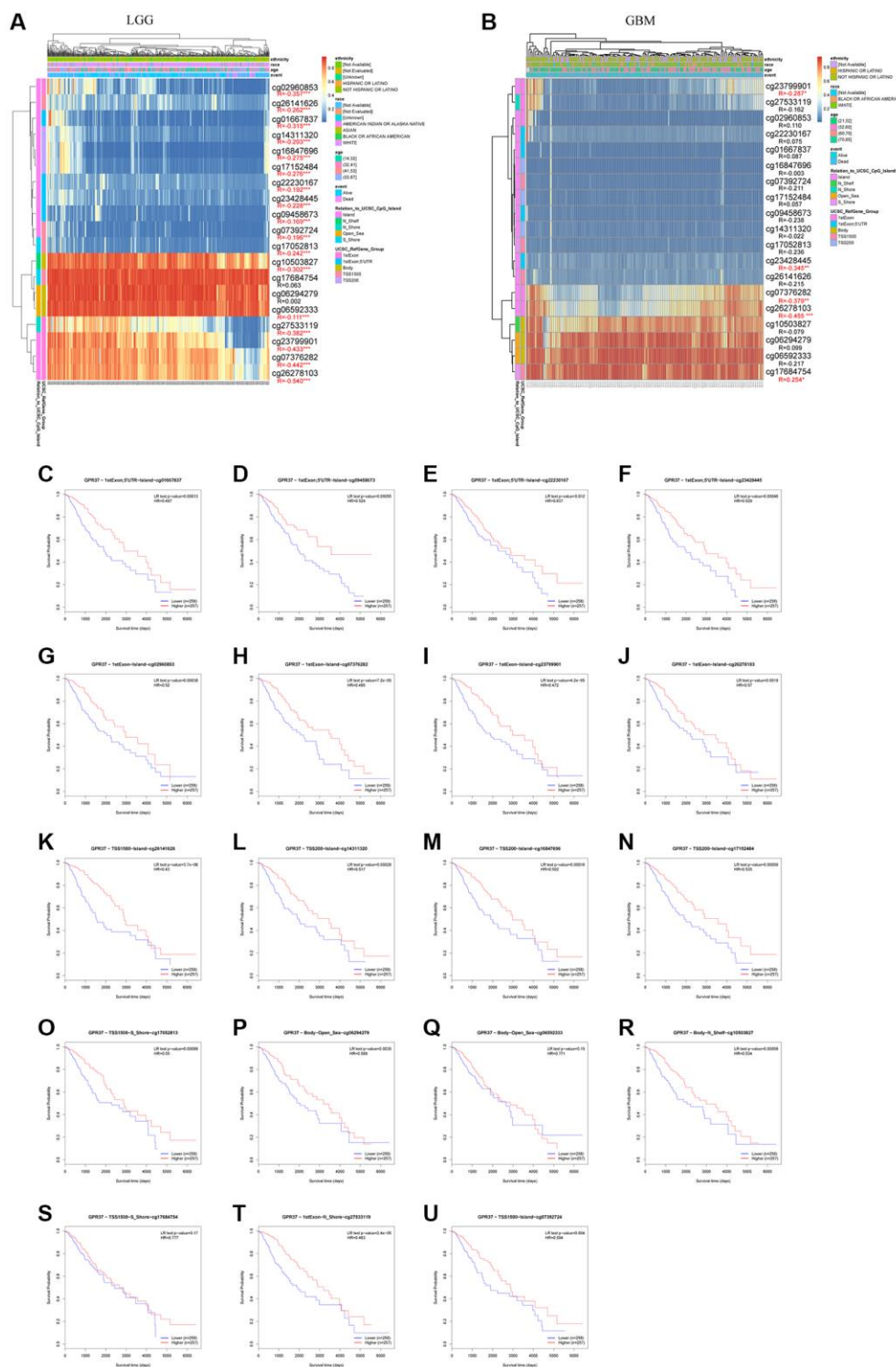


Figure 10. *GPR37* promoter methylation in glioma. (A, B) Waterfall plots showing the correlation methylation level of *GPR37* promoter and gene expression. (C–U) Survival curves as a function of methylation sites. * $P < 0.05$, ** $P < 0.01$, *** $P < 0.001$.

of macrophages, which are the most prominent inflammatory cells in tumor tissues [61]. The tumor-associated macrophages (TAMs) of the M1 phenotype promote inflammation, and inhibit tumor growth and invasion. The M2 macrophages on the other hand are anti-inflammatory and pro-tumorigenic [62, 63]. Glioma cells release a range of chemokines (CSF-1, MCP-1 and others) to recruit and activate TAMs, which then secrete the anti-inflammatory cytokines *IL-10* and *TGFBI* [64]. Furthermore, activation of *GPR37* in macrophages facilitates phagocytosis and the regression of inflammatory pain [65]. Bang and Qu et al. found that *GPR37*, the receptor of specialized pro-resolving mediators (SPMs), can bind to neuroprotectin D1 (*NPDI*) to inhibit the proinflammatory cytokine IL-1 and increase production of IL-10 and *TGFBI*. This polarizes the macrophages to the M2 phenotype and relieves inflammatory pain [66, 67]. Consistent with these reports, we found that the expression of *GPR37* was positively correlated with M2-like TAM markers, and higher proportion of M2 macrophages predicted worse prognosis in the *GPR37*^{high} patients. Thus, *GPR37* maybe contribute to glioma progression by recruiting TAMs and promoting M2 polarization.

Immune checkpoint inhibitors (ICIs) can effectively eliminate tumor cells by activating the anti-tumor immune responses [68, 69]. ICPs inhibit T cell function and survival by preventing antigen presentation, and overactivation of ICPs is a common strategy used by the tumor cells to avoid immune detection [70, 71]. The microenvironment of the CNS was long considered immunosuppressive due to the presence of the blood-brain barrier (BBB), and thus a major impediment to the use of ICIs in the treatment of gliomas [72]. Although this surmise has been challenged in recent years, a huge proportion of glioma patients fail to respond to ICIs. Therefore, it is crucial to identify the biomarkers of gliomas that may affect patient responsiveness to ICIs therapy [73]. We found that *GPR37* was positively correlated with several ICPs such as *CD274*, *PDCD1LG2*, *PDCD1*, *CD80*, *CD86*, *CTLA4*, *PVR*, *TIGIT*, *CD96*, *CD226*, *HAVCR2*, *LGALS9*, *CD47*, *SIPRA*, *CD200*, *CD200R1*, *CIITA* and *LAG3*, indicating that *GPR37* is a promising immune-related gene that can influence immunotherapy response in glioma patients.

DNA methylation is one of the variables of tumor growth [74, 75]. Promoter hypermethylation have been linked to reduced transcription or gene silencing, whereas hypermethylation of promoters leads to increased gene expression [76, 77]. In line with previous reports, we found that hypomethylation of the *GPR37* promoter was associated with increased

expression, and this result was more obvious in LGG than in GBM. Furthermore, LGG patients with hypermethylated promoter regions showed better prognosis. Therefore, the impact of specific *GPR37* methylation sites on gene expression and mortality, particularly in LGG patients, needs further investigation.

CONCLUSIONS

GPR37 is frequently overexpressed in glioma and is an independent prognostic predictor. It is involved in peroxisome control via the PPAR pathway, and is also associated with the infiltration of M2 macrophages and other immune cells. What is more, the overexpression of *GPR37* in glioma may be due to DNA hypomethylation. Our findings provide new insights into the possible mechanisms of glioma progression, particularly in the context of the tumor immune environment, which can help develop individualized treatment.

Abbreviations

aDCs: activated DCs; BBB: blood-brain barrier; CNS: central nervous system; DSS: disease-specific survival; GBM: glioblastoma; *GPR37*: G Protein-Coupled Receptor 37; GPCRs: G-protein-coupled receptors; GO: Gene Ontology; ICPs: immune checkpoints; ICIs: immune checkpoint inhibitors; iDCs: immature DCs; IHC: immunohistochemistry; KEGG: Kyoto Encyclopedia of Genes and Genomes; LGG: low-grade gliomas; OS: overall survival; pDCs: plasmacytoid DCs; ssGSEA: single-sample Gene Set Enrichment Analysis; TAMs: Tumor associated macrophages; TCGA: The Cancer Genome Atlas; Tcm: T central memory cells; Tem: T effector memory cells; Tfh: T follicular helper cells; Tgd: T gamma delta cells.

AUTHOR CONTRIBUTIONS

The study was conceived and designed by ZW, YW and KY. KL was involved in the methodology and investigation and prepared the primary figures and tables. Besides, ZW and KL participated in immunohistochemistry experiments. All authors participated to the drafting and revision of the paper, and read and approved the final manuscript.

ACKNOWLEDGMENTS

We acknowledge TCGA, and the numerous databases used in this study for providing us with such useful platforms and datasets that allowed us to complete this work.

CONFLICTS OF INTEREST

The authors declare no conflicts of interest related to this study.

ETHICAL STATEMENTS AND CONSENT

The authors declare that all methods were performed in accordance with the relevant guidelines and regulation. The findings include studies based on publicly available data from the TCGA, and other databases. The research involving human subjects was reviewed and approved by the Clinical Research and Applied Ethics Committee of the Second Affiliated Hospital of Guangzhou Medical University. The patient/participant provided written informed consent to participate in the study.

FUNDING

This work was supported by the National Natural Science Foundation of China (81901117), Natural Science Foundation of Guangdong Province (2019A1515010926) and National College Student Innovation and Entrepreneurship Training Program (202110570010), College Students' science and technology innovation project of Guangzhou Medical University (2020A024) and Health and Technology Project of Guangzhou (20211A010062), the Projects of Traditional Chinese Medicine Bureau of Guangdong Province (No. 20221242), the Special Fund for Hospital Pharmaceutical Research of Guangdong Province Hospital Association (grant number YXKY202201) and the Project of Traditional Chinese Medicine and Pharmacology of Guangzhou Municipal Health Commission (No. 20222A011017), Medical Scientific Research Foundation of Guangdong Province of China (No. A2021119).

REFERENCES

1. Wang L, Babikir H, Müller S, Yagnik G, Shamardani K, Catalan F, Kohanbash G, Alvarado B, Di Lullo E, Kriegstein A, Shah S, Wadhwa H, Chang SM, et al. The Phenotypes of Proliferating Glioblastoma Cells Reside on a Single Axis of Variation. *Cancer Discov.* 2019; 9:1708–19. <https://doi.org/10.1158/2159-8290.CD-19-0329> PMID:[31554641](https://pubmed.ncbi.nlm.nih.gov/31554641/)
2. Louis DN, Perry A, Wesseling P, Brat DJ, Cree IA, Figarella-Branger D, Hawkins C, Ng HK, Pfister SM, Reifenberger G, Soffiatti R, von Deimling A, Ellison DW. The 2021 WHO Classification of Tumors of the Central Nervous System: a summary. *Neuro Oncol.* 2021; 23:1231–51. <https://doi.org/10.1093/neuonc/noab106> PMID:[34185076](https://pubmed.ncbi.nlm.nih.gov/34185076/)
3. Xu S, Tang L, Li X, Fan F, Liu Z. Immunotherapy for glioma: Current management and future application. *Cancer Lett.* 2020; 476:1–12. <https://doi.org/10.1016/j.canlet.2020.02.002> PMID:[32044356](https://pubmed.ncbi.nlm.nih.gov/32044356/)
4. Gritsch S, Batchelor TT, Gonzalez Castro LN. Diagnostic, therapeutic, and prognostic implications of the 2021 World Health Organization classification of tumors of the central nervous system. *Cancer.* 2022; 128:47–58. <https://doi.org/10.1002/cncr.33918> PMID:[34633681](https://pubmed.ncbi.nlm.nih.gov/34633681/)
5. Leinartaitė L, Svenningsson P. Folding Underlies Bidirectional Role of GPR37/Pael-R in Parkinson Disease. *Trends Pharmacol Sci.* 2017; 38:749–60. <https://doi.org/10.1016/j.tips.2017.05.006> PMID:[28629580](https://pubmed.ncbi.nlm.nih.gov/28629580/)
6. Wang J, Xu M, Li DD, Abudukelimu W, Zhou XH. GPR37 promotes the malignancy of lung adenocarcinoma via TGF-β/Smad pathway. *Open Med (Wars).* 2020; 16:24–32. <https://doi.org/10.1515/med-2021-0011> PMID:[33364431](https://pubmed.ncbi.nlm.nih.gov/33364431/)
7. Wang H, Hu L, Zang M, Zhang B, Duan Y, Fan Z, Li J, Su L, Yan M, Zhu Z, Liu B, Yang Q. REG4 promotes peritoneal metastasis of gastric cancer through GPR37. *Oncotarget.* 2016; 7:27874–88. <https://doi.org/10.18632/oncotarget.8442> PMID:[27036049](https://pubmed.ncbi.nlm.nih.gov/27036049/)
8. Wang F, Zhao N, Gao G, Deng HB, Wang ZH, Deng LL, Yang Y, Lu C. Prognostic value of TP53 co-mutation status combined with EGFR mutation in patients with lung adenocarcinoma. *J Cancer Res Clin Oncol.* 2020; 146:2851–9. <https://doi.org/10.1007/s00432-020-03340-5> PMID:[32743759](https://pubmed.ncbi.nlm.nih.gov/32743759/)
9. Huang X, Wang Y, Nan X, He S, Xu X, Zhu X, Tang J, Yang X, Yao L, Wang X, Cheng C. The role of the orphan G protein-coupled receptor 37 (GPR37) in multiple myeloma cells. *Leuk Res.* 2014; 38: 225–35. <https://doi.org/10.1016/j.leukres.2013.11.007> PMID:[24290813](https://pubmed.ncbi.nlm.nih.gov/24290813/)
10. Zhang Y, Wang L. [Up-regulation of GPR37 promotes the proliferation of human glioma U251 cells]. *Xi Bao Yu Fen Zi Mian Yi Xue Za Zhi.* 2018; 34:341–5. PMID:[29973325](https://pubmed.ncbi.nlm.nih.gov/29973325/)
11. Li C, Tang Z, Zhang W, Ye Z, Liu F. GEPIA2021: integrating multiple deconvolution-based analysis into GEPIA. *Nucleic Acids Res.* 2021; 49:W242–6.

- <https://doi.org/10.1093/nar/gkab418>
PMID:34050758
12. Goldman MJ, Craft B, Hastie M, Repelka K, McDade F, Kamath A, Banerjee A, Luo Y, Rogers D, Brooks AN, Zhu J, Haussler D. Visualizing and interpreting cancer genomics data via the Xena platform. *Nat Biotechnol.* 2020; 38:675–8.
<https://doi.org/10.1038/s41587-020-0546-8>
PMID:32444850
 13. GTEx Consortium. The Genotype-Tissue Expression (GTEx) project. *Nat Genet.* 2013; 45:580–5.
<https://doi.org/10.1038/ng.2653>
PMID:23715323
 14. Cancer Genome Atlas Research Network. Comprehensive genomic characterization defines human glioblastoma genes and core pathways. *Nature.* 2008; 455:1061–8.
<https://doi.org/10.1038/nature07385>
PMID:18772890
 15. Pontén F, Jirstrom K, Uhlen M. The Human Protein Atlas—a tool for pathology. *J Pathol.* 2008; 216:387–93.
<https://doi.org/10.1002/path.2440>
PMID:18853439
 16. Prasad K, Prabhu GK. Image analysis tools for evaluation of microscopic views of immunohistochemically stained specimen in medical research—a review. *J Med Syst.* 2012; 36:2621–31.
<https://doi.org/10.1007/s10916-011-9737-7>
PMID:21584771
 17. Horai Y, Kakimoto T, Takemoto K, Tanaka M. Quantitative analysis of histopathological findings using image processing software. *J Toxicol Pathol.* 2017; 30:351–8.
<https://doi.org/10.1293/tox.2017-0031>
PMID:29097847
 18. Vasaikar SV, Straub P, Wang J, Zhang B. LinkedOmics: analyzing multi-omics data within and across 32 cancer types. *Nucleic Acids Res.* 2018; 46:D956–63.
<https://doi.org/10.1093/nar/gkx1090>
PMID:29136207
 19. Szklarczyk D, Gable AL, Nastou KC, Lyon D, Kirsch R, Pyysalo S, Doncheva NT, Legeay M, Fang T, Bork P, Jensen LJ, von Mering C. The STRING database in 2021: customizable protein-protein networks, and functional characterization of user-uploaded gene/measurement sets. *Nucleic Acids Res.* 2021; 49:D605–12.
<https://doi.org/10.1093/nar/gkaa1074>
PMID:33237311
 20. Shannon P, Markiel A, Ozier O, Baliga NS, Wang JT, Ramage D, Amin N, Schwikowski B, Ideker T. Cytoscape: a software environment for integrated models of biomolecular interaction networks. *Genome Res.* 2003; 13:2498–504.
<https://doi.org/10.1101/gr.1239303>
PMID:14597658
 21. Love MI, Huber W, Anders S. Moderated estimation of fold change and dispersion for RNA-seq data with DESeq2. *Genome Biol.* 2014; 15:550.
<https://doi.org/10.1186/s13059-014-0550-8>
PMID:25516281
 22. The Gene Ontology Consortium. The Gene Ontology Resource: 20 years and still GOing strong. *Nucleic Acids Res.* 2019; 47:D330–8.
<https://doi.org/10.1093/nar/gky1055>
PMID:30395331
 23. Kanehisa M, Goto S. KEGG: kyoto encyclopedia of genes and genomes. *Nucleic Acids Res.* 2000; 28:27–30.
<https://doi.org/10.1093/nar/28.1.27>
PMID:10592173
 24. Yu G, Wang LG, Han Y, He QY. clusterProfiler: an R package for comparing biological themes among gene clusters. *OMICS.* 2012; 16:284–7.
<https://doi.org/10.1089/omi.2011.0118>
PMID:22455463
 25. Subramanian A, Tamayo P, Mootha VK, Mukherjee S, Ebert BL, Gillette MA, Paulovich A, Pomeroy SL, Golub TR, Lander ES, Mesirov JP. Gene set enrichment analysis: a knowledge-based approach for interpreting genome-wide expression profiles. *Proc Natl Acad Sci U S A.* 2005; 102:15545–50.
<https://doi.org/10.1073/pnas.0506580102>
PMID:16199517
 26. Liberzon A, Birger C, Thorvaldsdottir H, Ghandi M, Mesirov JP, Tamayo P. The Molecular Signatures Database (MSigDB) hallmark gene set collection. *Cell Syst.* 2015; 1:417–25.
<https://doi.org/10.1016/j.cels.2015.12.004>
PMID:26771021
 27. Hänzelmann S, Castelo R, Guinney J. GSEA: gene set variation analysis for microarray and RNA-seq data. *BMC Bioinformatics.* 2013; 14:7.
<https://doi.org/10.1186/1471-2105-14-7>
PMID:23323831
 28. Bindea G, Mlecnik B, Tosolini M, Kirilovsky A, Waldner M, Obenauf AC, Angell H, Fredriksen T, Lafontaine L, Berger A, Bruneval P, Fridman WH, Becker C, et al. Spatiotemporal dynamics of intratumoral immune cells reveal the immune landscape in human cancer. *Immunity.* 2013; 39:782–95.
<https://doi.org/10.1016/j.immuni.2013.10.003>
PMID:24138885

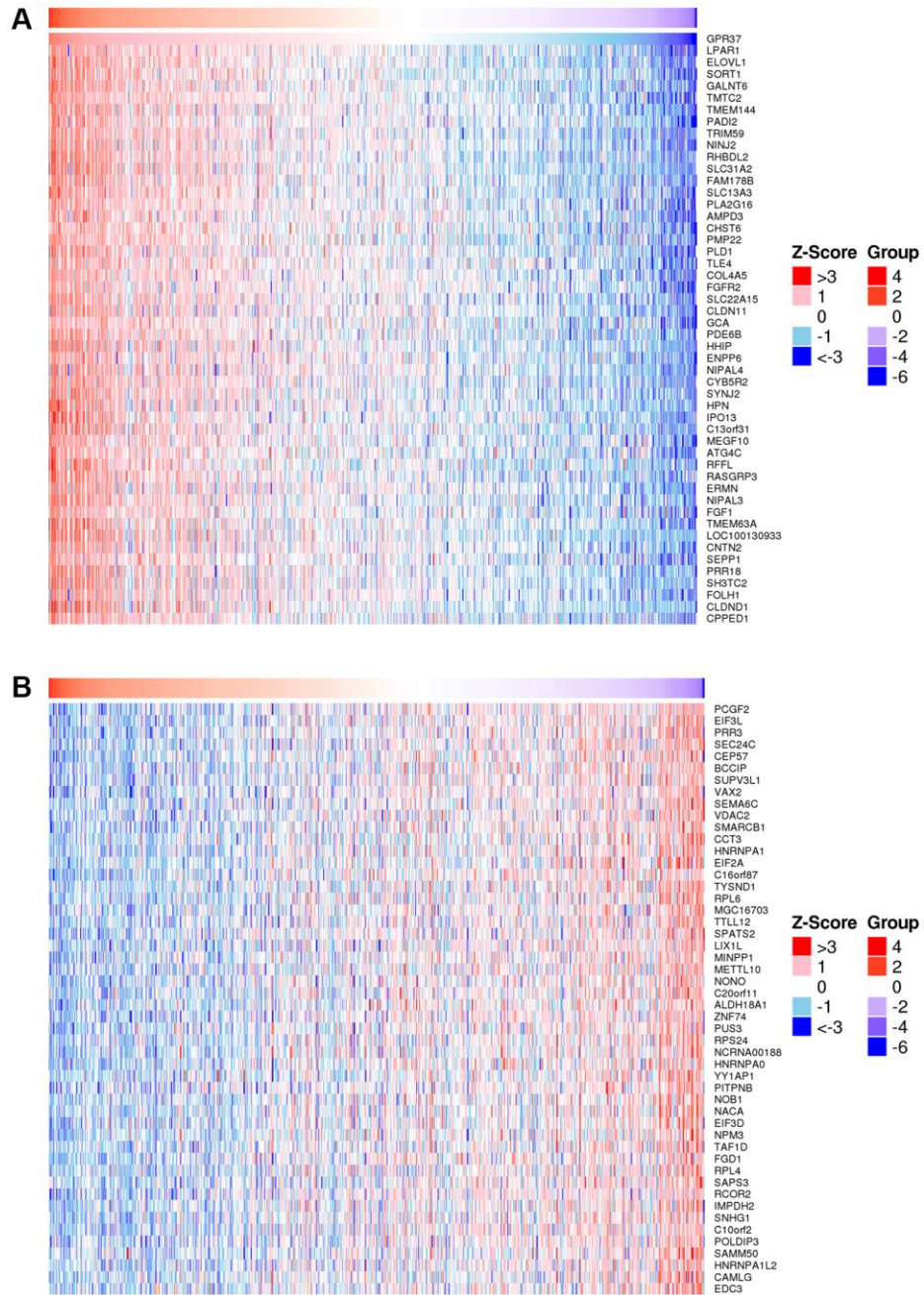
29. Li T, Fu J, Zeng Z, Cohen D, Li J, Chen Q, Li B, Liu XS. TIMER2.0 for analysis of tumor-infiltrating immune cells. *Nucleic Acids Res.* 2020; 48:W509–14. <https://doi.org/10.1093/nar/gkaa407> PMID:32442275
30. Modhukur V, Iljasenko T, Metsalu T, Lokk K, Laisk-Podar T, Vilo J. MethSurv: a web tool to perform multivariable survival analysis using DNA methylation data. *Epigenomics.* 2018; 10:277–88. <https://doi.org/10.2217/epi-2017-0118> PMID:29264942
31. Zakharova G, Efimov V, Raevskiy M, Rumiantsev P, Gudkov A, Belogurova-Ovchinnikova O, Sorokin M, Buzdin A. Reclassification of TCGA Diffuse Glioma Profiles Linked to Transcriptomic, Epigenetic, Genomic and Clinical Data, According to the 2021 WHO CNS Tumor Classification. *Int J Mol Sci.* 2022; 24:157. <https://doi.org/10.3390/ijms24010157> PMID:36613601
32. Bar-Shavit R, Maoz M, Kancharla A, Nag JK, Agranovich D, Grisaru-Granovsky S, Uziely B. G Protein-Coupled Receptors in Cancer. *Int J Mol Sci.* 2016; 17:1320. <https://doi.org/10.3390/ijms17081320> PMID:27529230
33. Dorsam RT, Gutkind JS. G-protein-coupled receptors and cancer. *Nat Rev Cancer.* 2007; 7:79–94. <https://doi.org/10.1038/nrc2069> PMID:17251915
34. Cecotka A, Polanska J. Region-Specific Methylation Profiling in Acute Myeloid Leukemia. *Interdiscip Sci.* 2018; 10:33–42. <https://doi.org/10.1007/s12539-018-0285-4> PMID:29405013
35. Chen W, Li W, Liu Z, Ma G, Deng Y, Li X, Wang Z, Zhou Q. Comprehensive analysis of competitive endogenous RNA associated with immune infiltration in lung adenocarcinoma. *Sci Rep.* 2021; 11:11056. <https://doi.org/10.1038/s41598-021-90755-w> PMID:34040139
36. Reichl B, Niederstaetter L, Boegl T, Neuditschko B, Bileck A, Gojo J, Buchberger W, Peyrl A, Gerner C. Determination of a Tumor-Promoting Microenvironment in Recurrent Medulloblastoma: A Multi-Omics Study of Cerebrospinal Fluid. *Cancers (Basel).* 2020; 12:1350. <https://doi.org/10.3390/cancers12061350> PMID:32466393
37. Mitsui J, Takahashi Y, Goto J, Tomiyama H, Ishikawa S, Yoshino H, Minami N, Smith DI, Lesage S, Aburatani H, Nishino I, Brice A, Hattori N, Tsuji S. Mechanisms of genomic instabilities underlying two common fragile-site-associated loci, PARK2 and DMD, in germ cell and cancer cell lines. *Am J Hum Genet.* 2010; 87:75–89. <https://doi.org/10.1016/j.ajhg.2010.06.006> PMID:20598272
38. Menezes J, Acquadro F, Wiseman M, Gómez-López G, Salgado RN, Talavera-Casañas JG, Buño I, Cervera JV, Montes-Moreno S, Hernández-Rivas JM, Ayala R, Calasanz MJ, Larrayoz MJ, et al. Exome sequencing reveals novel and recurrent mutations with clinical impact in blastic plasmacytoid dendritic cell neoplasm. *Leukemia.* 2014; 28:823–9. <https://doi.org/10.1038/leu.2013.283> PMID:24072100
39. Capurso G, Crnogorac-Jurcevic T, Milione M, Panzuto F, Campanini N, Downen SE, Di Florio A, Sette C, Bordi C, Lemoine NR, Delle Fave G. Peanut-like 1 (septin 5) gene expression in normal and neoplastic human endocrine pancreas. *Neuroendocrinology.* 2005; 81:311–21. <https://doi.org/10.1159/000088449> PMID:16179808
40. Gylfe AE, Kondelin J, Turunen M, Ristolainen H, Katainen R, Pitkänen E, Kaasinen E, Rantanen V, Tanskanen T, Varjosalo M, Lehtonen H, Palin K, Taipale M, et al. Identification of candidate oncogenes in human colorectal cancers with microsatellite instability. *Gastroenterology.* 2013; 145:540–3.e22. <https://doi.org/10.1053/j.gastro.2013.05.015> PMID:23684749
41. Kang SY, Halvorsen OJ, Grøvdal K, Bhattacharya N, Lee JM, Liu NW, Johnston BT, Johnston AB, Haukaas SA, Aamodt K, Yoo S, Akslen LA, Watnick RS. Prosaposin inhibits tumor metastasis via paracrine and endocrine stimulation of stromal p53 and Tsp-1. *Proc Natl Acad Sci U S A.* 2009; 106:12115–20. <https://doi.org/10.1073/pnas.0903120106> PMID:19581582
42. Mansi R, Fleischmann A, Mäcke HR, Reubi JC. Targeting GRPR in urological cancers—from basic research to clinical application. *Nat Rev Urol.* 2013; 10:235–44. <https://doi.org/10.1038/nrurol.2013.42> PMID:23507930
43. Gu Y, Liu Y, Fu L, Zhai L, Zhu J, Han Y, Jiang Y, Zhang Y, Zhang P, Jiang Z, Zhang X, Cao X. Tumor-educated B cells selectively promote breast cancer lymph node metastasis by HSPA4-targeting IgG. *Nat Med.* 2019; 25:312–22. <https://doi.org/10.1038/s41591-018-0309-y> PMID:30643287

44. Fan Y, Wang J, Jin W, Sun Y, Xu Y, Wang Y, Liang X, Su D. CircNR3C2 promotes HRD1-mediated tumor-suppressive effect via sponging miR-513a-3p in triple-negative breast cancer. *Mol Cancer*. 2021; 20:25. <https://doi.org/10.1186/s12943-021-01321-x> PMID:[33530981](https://pubmed.ncbi.nlm.nih.gov/33530981/)
45. Imai Y, Soda M, Inoue H, Hattori N, Mizuno Y, Takahashi R. An unfolded putative transmembrane polypeptide, which can lead to endoplasmic reticulum stress, is a substrate of Parkin. *Cell*. 2001; 105:891–902. [https://doi.org/10.1016/s0092-8674\(01\)00407-x](https://doi.org/10.1016/s0092-8674(01)00407-x) PMID:[11439185](https://pubmed.ncbi.nlm.nih.gov/11439185/)
46. Kitada T, Asakawa S, Hattori N, Matsumine H, Yamamura Y, Minoshima S, Yokochi M, Mizuno Y, Shimizu N. Mutations in the parkin gene cause autosomal recessive juvenile parkinsonism. *Nature*. 1998; 392:605–8. <https://doi.org/10.1038/33416> PMID:[9560156](https://pubmed.ncbi.nlm.nih.gov/9560156/)
47. Cockram PE, Kist M, Prakash S, Chen SH, Wertz IE, Vucic D. Ubiquitination in the regulation of inflammatory cell death and cancer. *Cell Death Differ*. 2021; 28:591–605. <https://doi.org/10.1038/s41418-020-00708-5> PMID:[33432113](https://pubmed.ncbi.nlm.nih.gov/33432113/)
48. Mattila SO, Tuusa JT, Petäjä-Repo UE. The Parkinson's-disease-associated receptor GPR37 undergoes metalloproteinase-mediated N-terminal cleavage and ectodomain shedding. *J Cell Sci*. 2016; 129:1366–77. <https://doi.org/10.1242/jcs.176115> PMID:[26869225](https://pubmed.ncbi.nlm.nih.gov/26869225/)
49. Dunham JH, Meyer RC, Garcia EL, Hall RA. GPR37 surface expression enhancement via N-terminal truncation or protein-protein interactions. *Biochemistry*. 2009; 48:10286–97. <https://doi.org/10.1021/bi9013775> PMID:[19799451](https://pubmed.ncbi.nlm.nih.gov/19799451/)
50. Morató X, Garcia-Esparcia P, Argerich J, Llorens F, Zerr I, Paslawski W, Borràs E, Sabidó E, Petäjä-Repo UE, Fernández-Dueñas V, Ferrer I, Svenningsson P, Ciruela F. Ecto-GPR37: a potential biomarker for Parkinson's disease. *Transl Neurodegener*. 2021; 10:8. <https://doi.org/10.1186/s40035-021-00232-7> PMID:[33637132](https://pubmed.ncbi.nlm.nih.gov/33637132/)
51. Dahabieh MS, Di Pietro E, Jangal M, Goncalves C, Witcher M, Braverman NE, Del Rincón SV. Peroxisomes and cancer: The role of a metabolic specialist in a disease of aberrant metabolism. *Biochim Biophys Acta Rev Cancer*. 2018; 1870:103–21. <https://doi.org/10.1016/j.bbcan.2018.07.004> PMID:[30012421](https://pubmed.ncbi.nlm.nih.gov/30012421/)
52. Lodhi IJ, Semenkovich CF. Peroxisomes: a nexus for lipid metabolism and cellular signaling. *Cell Metab*. 2014; 19:380–92. <https://doi.org/10.1016/j.cmet.2014.01.002> PMID:[24508507](https://pubmed.ncbi.nlm.nih.gov/24508507/)
53. Mirza AZ, Althagafi II, Shamshad H. Role of PPAR receptor in different diseases and their ligands: Physiological importance and clinical implications. *Eur J Med Chem*. 2019; 166:502–13. <https://doi.org/10.1016/j.ejmech.2019.01.067> PMID:[30739829](https://pubmed.ncbi.nlm.nih.gov/30739829/)
54. Dean JM, Lodhi IJ. Structural and functional roles of ether lipids. *Protein Cell*. 2018; 9:196–206. <https://doi.org/10.1007/s13238-017-0423-5> PMID:[28523433](https://pubmed.ncbi.nlm.nih.gov/28523433/)
55. Di Giacomo E, Benedetti E, Cristiano L, Antonosante A, d'Angelo M, Fidoamore A, Barone D, Moreno S, Ippoliti R, Cerù MP, Giordano A, Cimini A. Roles of PPAR transcription factors in the energetic metabolic switch occurring during adult neurogenesis. *Cell Cycle*. 2017; 16:59–72. <https://doi.org/10.1080/15384101.2016.1252881> PMID:[27860527](https://pubmed.ncbi.nlm.nih.gov/27860527/)
56. Nwankwo JO, Robbins ME. Peroxisome proliferator-activated receptor- gamma expression in human malignant and normal brain, breast and prostate-derived cells. *Prostaglandins Leukot Essent Fatty Acids*. 2001; 64:241–5. <https://doi.org/10.1054/plf.2001.0266> PMID:[11418018](https://pubmed.ncbi.nlm.nih.gov/11418018/)
57. Khoo NK, Hebbar S, Zhao W, Moore SA, Domann FE, Robbins ME. Differential activation of catalase expression and activity by PPAR agonists: implications for astrocyte protection in anti-glioma therapy. *Redox Biol*. 2013; 1:70–9. <https://doi.org/10.1016/j.redox.2012.12.006> PMID:[24024139](https://pubmed.ncbi.nlm.nih.gov/24024139/)
58. Gupta G, Singhvi G, Chellappan DK, Sharma S, Mishra A, Dahiya R, de Jesus Andreoli Pinto T, Dua K. Peroxisome proliferator-activated receptor gamma: promising target in glioblastoma. *Panminerva Med*. 2018; 60:109–16. <https://doi.org/10.23736/S0031-0808.18.03462-6> PMID:[30176701](https://pubmed.ncbi.nlm.nih.gov/30176701/)
59. Greten FR, Grivennikov SI. Inflammation and Cancer: Triggers, Mechanisms, and Consequences. *Immunity*. 2019; 51:27–41. <https://doi.org/10.1016/j.immuni.2019.06.025> PMID:[31315034](https://pubmed.ncbi.nlm.nih.gov/31315034/)
60. Wei J, Chen P, Gupta P, Ott M, Zamler D, Kassab C, Bhat KP, Curran MA, de Groot JF, Heimberger AB. Immune biology of glioma-associated macrophages

- and microglia: functional and therapeutic implications. *Neuro Oncol.* 2020; 22:180–94.
<https://doi.org/10.1093/neuonc/noz212>
PMID:[31679017](https://pubmed.ncbi.nlm.nih.gov/31679017/)
61. Guerriero JL. Macrophages: The Road Less Traveled, Changing Anticancer Therapy. *Trends Mol Med.* 2018; 24:472–89.
<https://doi.org/10.1016/j.molmed.2018.03.006>
PMID:[29655673](https://pubmed.ncbi.nlm.nih.gov/29655673/)
62. Locati M, Curtale G, Mantovani A. Diversity, Mechanisms, and Significance of Macrophage Plasticity. *Annu Rev Pathol.* 2020; 15:123–47.
<https://doi.org/10.1146/annurev-pathmechdis-012418-012718>
PMID:[31530089](https://pubmed.ncbi.nlm.nih.gov/31530089/)
63. Yunna C, Mengru H, Lei W, Weidong C. Macrophage M1/M2 polarization. *Eur J Pharmacol.* 2020; 877:173090.
<https://doi.org/10.1016/j.ejphar.2020.173090>
PMID:[32234529](https://pubmed.ncbi.nlm.nih.gov/32234529/)
64. Hambardzumyan D, Gutmann DH, Kettenmann H. The role of microglia and macrophages in glioma maintenance and progression. *Nat Neurosci.* 2016; 19:20–7.
<https://doi.org/10.1038/nn.4185>
PMID:[26713745](https://pubmed.ncbi.nlm.nih.gov/26713745/)
65. Bang S, Donnelly CR, Luo X, Toro-Moreno M, Tao X, Wang Z, Chandra S, Bortsov AV, Derbyshire ER, Ji RR. Activation of GPR37 in macrophages confers protection against infection-induced sepsis and pain-like behaviour in mice. *Nat Commun.* 2021; 12:1704.
<https://doi.org/10.1038/s41467-021-21940-8>
PMID:[33731716](https://pubmed.ncbi.nlm.nih.gov/33731716/)
66. Bang S, Xie YK, Zhang ZJ, Wang Z, Xu ZZ, Ji RR. GPR37 regulates macrophage phagocytosis and resolution of inflammatory pain. *J Clin Invest.* 2018; 128:3568–82.
<https://doi.org/10.1172/JCI99888>
PMID:[30010619](https://pubmed.ncbi.nlm.nih.gov/30010619/)
67. Qu L, Caterina MJ. Accelerating the reversal of inflammatory pain with NPD1 and its receptor GPR37. *J Clin Invest.* 2018; 128:3246–9.
<https://doi.org/10.1172/JCI122203>
PMID:[30010628](https://pubmed.ncbi.nlm.nih.gov/30010628/)
68. Gibney GT, Weiner LM, Atkins MB. Predictive biomarkers for checkpoint inhibitor-based immunotherapy. *Lancet Oncol.* 2016; 17:e542–51.
[https://doi.org/10.1016/S1470-2045\(16\)30406-5](https://doi.org/10.1016/S1470-2045(16)30406-5)
PMID:[27924752](https://pubmed.ncbi.nlm.nih.gov/27924752/)
69. Abril-Rodriguez G, Ribas A. SnapShot: Immune Checkpoint Inhibitors. *Cancer Cell.* 2017; 31:848.e1.
<https://doi.org/10.1016/j.ccell.2017.05.010>
PMID:[28609660](https://pubmed.ncbi.nlm.nih.gov/28609660/)
70. Sun C, Mezzadra R, Schumacher TN. Regulation and Function of the PD-L1 Checkpoint. *Immunity.* 2018; 48:434–52.
<https://doi.org/10.1016/j.immuni.2018.03.014>
PMID:[29562194](https://pubmed.ncbi.nlm.nih.gov/29562194/)
71. Elliot TAE, Jennings EK, Lecky DAJ, Thawait N, Flores-Langarica A, Copland A, Maslowski KM, Wraith DC, Bending D. Antigen and checkpoint receptor engagement recalibrates T cell receptor signal strength. *Immunity.* 2021; 54:2481–96.e6.
<https://doi.org/10.1016/j.immuni.2021.08.020>
PMID:[34534438](https://pubmed.ncbi.nlm.nih.gov/34534438/)
72. Daubon T, Hemadou A, Romero Garmendia I, Saleh M. Glioblastoma Immune Landscape and the Potential of New Immunotherapies. *Front Immunol.* 2020; 11:585616.
<https://doi.org/10.3389/fimmu.2020.585616>
PMID:[33154756](https://pubmed.ncbi.nlm.nih.gov/33154756/)
73. Qi Y, Liu B, Sun Q, Xiong X, Chen Q. Immune Checkpoint Targeted Therapy in Glioma: Status and Hopes. *Front Immunol.* 2020; 11:578877.
<https://doi.org/10.3389/fimmu.2020.578877>
PMID:[33329549](https://pubmed.ncbi.nlm.nih.gov/33329549/)
74. Morgan AE, Davies TJ, Mc Auley MT. The role of DNA methylation in ageing and cancer. *Proc Nutr Soc.* 2018; 77:412–22.
<https://doi.org/10.1017/S0029665118000150>
PMID:[29708096](https://pubmed.ncbi.nlm.nih.gov/29708096/)
75. Greenberg MVC, Bourc'his D. The diverse roles of DNA methylation in mammalian development and disease. *Nat Rev Mol Cell Biol.* 2019; 20:590–607.
<https://doi.org/10.1038/s41580-019-0159-6>
PMID:[31399642](https://pubmed.ncbi.nlm.nih.gov/31399642/)
76. Jones PA. Functions of DNA methylation: islands, start sites, gene bodies and beyond. *Nat Rev Genet.* 2012; 13:484–92.
<https://doi.org/10.1038/nrg3230>
PMID:[22641018](https://pubmed.ncbi.nlm.nih.gov/22641018/)
77. Van Tongelen A, Lorient A, De Smet C. Oncogenic roles of DNA hypomethylation through the activation of cancer-germline genes. *Cancer Lett.* 2017; 396:130–7.
<https://doi.org/10.1016/j.canlet.2017.03.029>
PMID:[28342986](https://pubmed.ncbi.nlm.nih.gov/28342986/)

SUPPLEMENTARY MATERIALS

Supplementary Figure



Supplementary Figure 1. Co-expression and gene set enrichment analysis in glioma. (A) Heatmap of the 50 negatively correlated genes of *GPR37*. (B) Heatmap of the top 50 positively correlated genes of *GPR37*.

Supplementary Tables

Please browse Full Text version to see the data of Supplementary Table 1.

Supplementary Table 1. The clinical data and molecular data of all glioma samples. Abbreviations: OS: overall survival; DSS: disease specific survival; Homdel: Homozygous deletion; IDH: Isocitrate dehydrogenase; WT: wildtype; Mut: mutant.

Supplementary Table 2. The clinicopathological variables of 38 patients.

Characteristics	Total (N)
Grade, <i>n</i> (%)	
G2 & G3	9 (23.7%)
G4	29 (76.3%)
Histological type, <i>n</i> (%)	
Oligodendroglioma, IDH mut, 1p/19q code1	4 (10.5%)
Astrocytoma, IDH mut	10 (26.3%)
Glioblastoma	24 (63.2%)
Gender, <i>n</i> (%)	
Male	22 (57.9%)
Female	16 (42.1%)
Age, <i>n</i> (%)	
≤60	27 (71.1%)
>60	11 (28.9%)

Supplementary Table 3. Cox analysis of GPR37 expression and other clinicopathological variables for OS (univariate and multivariate).

Characteristics	Total (N)	HR (95% CI) Univariate analysis (OS)	<i>P</i> value Univariate analysis	HR (95% CI) Multivariate analysis (OS)	<i>P</i> value Multivariate analysis
GPR37	698		<0.001		
Low	351	Reference		Reference	
High	347	1.851 (1.450–2.362)	<0.001	1.771 (1.180–2.658)	0.006
Grade	695		<0.001		
G4	284	Reference		Reference	
G2 & G3	411	0.116 (0.088–0.153)	<0.001	2.482 (0.962–6.405)	0.060
Histological Type	688		<0.001		
Glioblastoma, IDH wildtype	246	Reference		Reference	
Oligodendroglioma, IDH mutation, 1p/19q-code1	171	0.081 (0.052–0.125)	<0.001	0.130 (0.048–0.354)	<0.001
Astrocytoma, IDH mutation	271	0.137 (0.103–0.184)	<0.001	0.211 (0.090–0.494)	<0.001
CDKN2A/B homdel	698		<0.001		
Non-homdel	549	Reference		Reference	
Homdel	149	5.332 (4.123–6.896)	<0.001	4.770 (2.617–8.694)	<0.001
Age	698		<0.001		
≤60	555	Reference		Reference	
>60	143	4.696 (3.620–6.093)	<0.001	4.189 (2.639–6.650)	<0.001

Gender	698		0.071		
Male	401	Reference			
Female	297	0.800 (0.627–1.021)	0.073		
Primary therapy outcome	464		<0.001		
PR & CR	204	Reference		Reference	
PD & SD	260	4.868 (2.783–8.514)	<0.001	4.000 (2.268–7.055)	<0.001

Supplementary Table 4. Cox analysis of GPR37 expression and other clinicopathological variables for DSS (univariate and multivariate).

Characteristics	Total (N)	HR (95% CI) Univariate analysis (DSS)	P value Univariate analysis	HR (95% CI) Multivariate analysis (DSS)	P value Multivariate analysis
GPR37	677		<0.001		
Low	339	Reference		Reference	
High	338	2.031 (1.565–2.637)	<0.001	1.834 (1.196–2.813)	0.005
Grade	674		<0.001		
G4	270	Reference		Reference	
G2 & G3	404	0.105 (0.078–0.141)	<0.001	2.427 (0.926–6.364)	0.071
Histological Type	667		<0.001		
Glioblastoma, IDH wildtype	232	Reference		Reference	
Oligodendroglioma, IDH mutation, 1p/19q-codel	170	0.071 (0.044–0.115)	<0.001	0.112 (0.040–0.315)	<0.001
Astrocytoma, IDH mutation	265	0.133 (0.098–0.182)	<0.001	0.199 (0.085–0.468)	<0.001
CDKN2A/B homdel	677		<0.001		
Non-homdel	537	Reference		Reference	
Homdel	140	5.457 (4.167–7.147)	<0.001	4.716 (2.573–8.646)	<0.001
Age	677		<0.001		
≤60	544	Reference		Reference	
>60	133	4.528 (3.430–5.978)	<0.001	3.815 (2.352–6.190)	<0.001
Gender	677		0.104		
Male	388	Reference			
Female	289	0.809 (0.625–1.047)	0.107		
Primary therapy outcome	460		<0.001		
PR & CR	204	Reference		Reference	
PD & SD	256	5.486 (3.009–10.001)	<0.001	4.442 (2.412–8.182)	<0.001

Supplementary Table 5. Gene enrichment study based on the phenotypes of high and low GPR37 expression.

Gene set name	NES
High expression	
GO_NEGATIVE_REGULATION_OF_T_CELL_RECEPTOR_SIGNALING_PATHWAY	1.766
GO_REGULATION_OF_MACROPHAGE_DERIVED_FOAM_CELL_DIFFERENTIATION	1.737
GO_LEUKOCYTE_PROLIFERATION	1.69
GO_B_CELL_PROLIFERATION	1.668
GO_MYELOID_LEUKOCYTE_DIFFERENTIATION	1.612
KEGG_NEUROACTIVE_LIGAND_RECEPTOR_INTERACTION	1.754

KEGG_CALCIIUM_SIGNALING_PATHWAY	1.654
KEGG_B_CELL_RECEPTOR_SIGNALING_PATHWAY	1.621
KEGG_PPAR_SIGNALING_PATHWAY	1.612
KEGG_TOLL_LIKE_RECEPTOR_SIGNALING_PATHWAY	1.608
<hr/>	
Low expression	
GO_HUMORAL_IMMUNE_RESPONSE_MEDIATED_BY_CIRCULATING_IMMUNOGLOBULIN	-3.223
GO_IMMUNOGLOBULIN_RECEPTOR_BINDING	-3.357
GO_ANTIGEN_BINDING	-3.36
GO_IMMUNOGLOBULIN_COMPLEX_CIRCULATING	-3.37
GO_IMMUNOGLOBULIN_COMPLEX	-3.678
KEGG_OXIDATIVE_PHOSPHORYLATION	-1.469
KEGG_SPLICEOSOME	-1.626
KEGG_RIBOSOME	-3.092
<hr/>	